

Supplementary Materials for

395

A Candida auris-specific adhesin, SCF1, governs surface association and colonization

Darian J. Santana, Juliet A. E. Anku, Guolei Zhao, Robert Zarnowski, Chad J. Johnson, Haley Hautau, Noelle D. Visser, Ashraf S. Ibrahim, David Andes, Jeniel E. Nett, Shakti Singh, Teresa R. O'Meara

400

Correspondence to: tromeara@umich.edu

This PDF file includes:

405

Materials and Methods
Figs. S1 to S15
Tables S1 to S5
Captions for Data S1

410

Other Supplementary Materials for this manuscript include the following:

Data S1 Source Data

415

Materials and Methods

Strains and Culture Conditions

420 A list of all strains used in this study is included in Table S3. Clinical *C. auris* isolates were obtained through the CDC/FDA Antibiotic Resistant Isolate Bank (50) or from Rush University Medical Center, Chicago, IL (Gift from Mary Hayden). Except where specified, *C. auris* cells were cultured at 30 °C in YPD liquid media (1% yeast extract, 2% peptone, 2% dextrose) with constant agitation. All strains were maintained as frozen stocks of 25% glycerol at -80 °C.

Genomic DNA Isolation

425 Genomic DNA was isolated using a PCA extraction method. Briefly, yeast cells were incubated overnight in liquid YPD at 30°C then harvested by centrifugation and resuspended in lysis buffer (2% (v/v) Triton X-100, 1% (w/v) SDS, 100 mM NaCl, 10 mM Tris-Cl, 1 mM EDTA). The cell suspension was disrupted by bead-beating and released DNA was extracted into PCA and then into Chloroform. The resulting DNA was purified by ethanol precipitation and resuspended in water before being treated with RNase A. RNase was heat-inactivated, then extracted DNA was purified by ethanol precipitation and resuspended in water.

Primers and Plasmids

430 A list of all plasmids used in this study is included in Table S4. A list of all primers used in this study is included in Table S5. Cassettes for transformation of *C. auris* were maintained in the multiple cloning site of the pUC19 cloning vector and assembled from fragments using the NeBuilder HIFI DNA Assembly Master Mix (NEB #E2621) or the Codex DNA Gibson Assembly Ultra Master Mix (Codex DNA #GA1200) according to the manufacturer's instructions.

Plasmid and Strain Construction

440 **pTO144/CauTO186:** The plasmid backbone was amplified from pTO139 using oTO190-oTO191. The NAT cassette was amplified from pTO137 using oTO186-oTO187. The NAT cassette was flanked by approximately 500 bp regions homologous to the regions immediately upstream and downstream of *ALS* (B9J08_002582) amplified from *C. auris* genomic DNA using oTO184-oTO185 and oTO188-oTO189 respectively. The repair cassette was amplified using oTO18-oTO19 and transformed into AR0382 to generate CauTO186.

450 **pTO167/CauTO187:** The plasmid backbone was amplified from pTO139 using oTO410-oTO411. The NAT cassette was amplified from pTO137 using oTO414-oTO415. The NAT cassette was flanked by approximately 500 bp regions homologous to the regions immediately upstream and downstream of *ALS* (B9J08_004498) amplified from *C. auris* genomic DNA using oTO412-oTO413 and oTO416-oTO417 respectively. The repair cassette was amplified using oTO18-oTO19 and transformed into AR0382 to generate CauTO187.

460 **pTO166/CauTO226:** The plasmid backbone was amplified from pTO139 using oTO402-oTO403. The NAT cassette was amplified from pTO137 using oTO406-oTO407. The NAT cassette was flanked by approximately 500 bp regions homologous to the regions immediately upstream and downstream of *ALS* (B9J08_004112) amplified from *C. auris* genomic DNA using oTO404-oTO404 and oTO408-oTO409 respectively. The repair cassette was amplified using oTO18-oTO19 and transformed into AR0382 to generate CauTO226.

465 **pTO145/CauTO233:** The plasmid backbone was amplified from pTO139 using oTO198-oTO199. The NAT cassette was amplified from pTO137 using oTO194-oTO195. The NAT cassette was flanked by approximately 500 bp regions homologous to the regions immediately upstream and downstream of *IFF* (B9J08_004100) amplified from *C. auris* genomic DNA using oTO192-oTO193 and oTO196-oTO197 respectively. The repair cassette was amplified using oTO18-oTO19 and transformed into AR0382 to generate CauTO233.

470 **pTO148/CauTO234:** The plasmid backbone was amplified from pTO139 using oTO222-oTO223. The NAT cassette was amplified from pTO137 using oTO218-oTO219. The NAT cassette was flanked by approximately 500 bp regions homologous to the regions immediately upstream and downstream of *IFF* (B9J08_004109) amplified from *C. auris* genomic DNA using oTO216-oTO217 and oTO220-oTO221 respectively. The repair cassette was amplified using oTO18-oTO19 and transformed into AR0382 to generate CauTO234.

475 **pTO202/CauTO235:** The plasmid backbone was amplified from pTO139 using oTO590-oTO591. The NAT cassette was amplified from pTO137 using oTO788-oTO789. The NAT cassette was flanked by approximately 500 bp regions homologous to the regions immediately upstream and downstream of *IFF* (B9J08_004098) amplified from *C. auris* genomic DNA using oTO786-oTO787 and oTO790-oTO791 respectively. The repair cassette was amplified using oTO18-oTO19 and transformed into AR0382 to generate CauTO235.

480 **pTO188/CauTO236:** The plasmid backbone was amplified from pTO139 using oTO590-oTO591. The NEO cassette was amplified from pTO169 using oTO668-oTO669. The NEO cassette was flanked by approximately 500 bp regions homologous to the regions immediately upstream and downstream of *IFF* (B9J08_004110) amplified from *C. auris* genomic DNA using oTO678-oTO679 and oTO680-oTO681 respectively. The repair cassette was amplified using oTO18-oTO19 and transformed into AR0382 to generate CauTO236.

485 **pTO146/CauTO247:** The plasmid backbone was amplified from pTO139 using oTO206-oTO207. The NAT cassette was amplified from pTO137 using oTO202-oTO203. The NAT cassette was flanked by approximately 500 bp regions homologous to the regions immediately upstream and downstream of *IFF* (B9J08_001531) amplified from *C. auris* genomic DNA using oTO200-oTO201 and oTO204-oTO205 respectively. The repair cassette was amplified using oTO18-oTO19 and transformed into AR0382 to generate CauTO247.

495 **pTO147/CauTO248:** The plasmid backbone was amplified from pTO139 using oTO214-oTO215. The NAT cassette was amplified from pTO137 using oTO210-oTO211. The NAT cassette was flanked by approximately 500 bp regions homologous to the regions immediately upstream and downstream of *IFF* (B9J08_004892) amplified from *C. auris* genomic DNA using oTO208-oTO209 and oTO212-oTO213 respectively. The repair cassette was amplified using oTO18-oTO19 and transformed into AR0382 to generate CauTO248.

505 **pTO205/CauTO249:** The plasmid backbone was amplified from pTO139 using oTO590-oTO591. The NAT cassette was amplified from pTO137 using oTO821-oTO822. The NAT cassette was flanked by approximately 500 bp regions homologous to the regions immediately upstream and downstream of *IFF* (B9J08_001155) amplified from *C. auris* genomic DNA using

510

oTO819-oTO820 and oTO823-oTO824 respectively. The repair cassette was amplified using oTO18-oTO19 and transformed into AR0382 to generate CauTO249.

515 **pTO206/CauTO250:** The plasmid backbone was amplified from pTO139 using oTO590-oTO591. The NAT cassette was amplified from pTO137 using oTO827-oTO828. The NAT cassette was flanked by approximately 500 bp regions homologous to the regions immediately upstream and downstream of *IFF* (B9J08_004451) amplified from *C. auris* genomic DNA using oTO825-TO826 and oTO829-oTO830 respectively. The repair cassette was amplified using oTO18-oTO19 and transformed into AR0382 to generate CauTO250.

520 **pTO207/CauTO251:** The plasmid backbone was amplified from pTO139 using oTO590-oTO591. The NAT cassette was amplified from pTO137 using oTO833-oTO834. The NAT cassette was flanked by approximately 500 bp regions homologous to the regions immediately upstream and downstream of *IFF* (B9J08_000675) amplified from *C. auris* genomic DNA using oTO831-TO832 and oTO835-oTO836 respectively. The repair cassette was amplified using oTO18-oTO19 and transformed into AR0382 to generate CauTO250.

530 **pTO211/CauTO261:** The plasmid backbone was amplified from pTO139 using oTO590-oTO591. The NAT cassette was amplified from pTO137 using oTO668-oTO874. The NAT cassette was flanked by approximately 500 bp regions homologous to the regions immediately upstream and downstream of *SCF1* (B9J08_001458) amplified from *C. auris* genomic DNA using oTO879-TO880 and oTO881-oTO882 respectively. The repair cassette was amplified using oTO18-oTO19 and transformed into AR0382 to generate CauTO261.

535 **CauTO320:** A FLAG-tagged *SCF1* complementation cassette was generated using overlap extension PCR to insert a FLAG sequence between domains A and B (between amino acids 250-251). Fragments were amplified from pTO223 using oTO1160-oTO224 and oTO1159-oTO225 and fused with extension primers oTO945-oTO946. The resulting fusion fragment was transformed into CauTO261 to generate CauTO320.

540 **pTO222/CauTO307:** The ORF for *IFF* (B9J08_004109) along with approximately 500 bp of upstream sequence was amplified from *C. auris* genomic DNA using oTO937-oTO938. The NEO cassette was amplified from pTO169 using oTO668-oTO669. The plasmid backbone was amplified from pTO139 using oTO943-oTO944. The repair cassette was amplified using oTO947-oTO948 and transformed into CauTO234 to generate CauTO307.

545 **pTO221/CauTO270:** The vector including approximately 500 bp regions homologous to the regions immediately upstream and downstream of *IFF* (B9J08_004109) was amplified from pTO148 using oTO927-oTO928. The NEO cassette was amplified from pTO169 using oTO668-oTO669. The repair cassette was amplified using oTO18-oTO19 and transformed into CauTO261 to generate CauTO270.

555 **CaTO227:** The *ALS1* deletion cassette with NAT was amplified from pTO100 using oTO652-oTO653. The sgRNA guide was amplified from pTO102 usint oTO6-oTO698 and oTO8-oTO699, and the fusion was amplified using oTO7-oTO9. Cas9 was amplified from pTO102 using oTO40-oTO41. The three linear pieces of DNA were transformed into SC5314 using a PEG-heat shock transformation, as described previously (51).

560 **pTO288/CauTO436:** The plasmid backbone was amplified from pTO139 using oTO590-oTO591. The NAT cassette and pCauTEF1 promoter were amplified from pTO250 using oTO1482-oTO1483. Flanking regions of approximately 500 bp were amplified from *C. auris* genomic DNA using oTO1480-oTO1481 and oTO1484-oTO1485. The repair cassette was amplified using oTO18-19 and transformed into AR0382 to generate CauTO436.

565 **pTO255/ChTO346:** The plasmid backbone was amplified from pTO139 using oTO590-oTO591. The NAT cassette was amplified from pTO137 using oTO668-oTO874. The NAT cassette was flanked by approximately 500 bp regions homologous to the regions immediately upstream and downstream of *SCF1* (CXQ85_003100) amplified from *C. haemulonii* genomic DNA using oTO1223-oTO1224 and oTO1225-oTO1226 respectively. The repair cassette was amplified using oTO18-oTO19 and transformed into AR0395 to generate ChTO346.

570 **pTO264/CauTO364:** The plasmid backbone was amplified from pTO139 using oTO590-oTO591. *C. haemulonii SCF1* was amplified from AR0395 gDNA using oTO1276-oTO1277. The ADH1 terminator, NEO cassette, and approximately 500 bp of *SCF1* downstream intragenic region were amplified from pTO223 using oTO1274-oTO882. Approximately 500 bp *SCF1* upstream flanking region was amplified from *C. auris* gDNA using oTO879-oTO1275. The repair cassette was amplified using oTO945-946 and transformed into CauTO261 to generate CauTO364.

580 **pTO250/CauTO308, CauTO312, CauTO323:** The plasmid backbone was amplified from pTO139 using oTO590-oTO591. Approximately 500 bp homologous to the region immediately upstream of *SCF1* (B9J08_001458) was amplified from *C. auris* genomic DNA using oTO879-oTO1150. The NAT cassette was amplified from pTO137 using oTO668-oTO875. 1000 bp of promoter sequence upstream of *CauTEF1* (B9J08_003610) was amplified from *C. auris* genomic DNA using oTO1151-1152. The first 506 bp of the *SCF1* ORF was amplified using oTO1153-oTO1154. The repair cassette was amplified using oTO945-oTO1161 and transformed into AR0387 to generate CauTO308 and into AR0381 to generate CauTO312. The entire promoter replacement cassette and *SCF1* ORF was amplified from CauTO308 genomic DNA using oTO945-oTO946 and transformed into AR0381 to generate CauTO323.

590 **pTO223/CauTO306:** The ORF for *SCF1* (B9J08_001458) along with approximately 500 bp of upstream sequence was amplified from *C. auris* genomic DNA using oTO879-oTO1078. The ADH1 terminator and NEO cassette were amplified from pTO169 using oTO1066-oTO668. Approximately 500 bp homologous to the region immediately downstream of *SCF1* was amplified from *C. auris* genomic DNA using oTO1077-oTO882. The plasmid backbone was amplified from pTO139 using oTO590-oTO591. The repair cassette was amplified using oTO945-oTO946 and transformed into CauTO261 to generate CauTO306.

600 **pTO284/CauTO438:** *SCF1* was amplified from AR0381 gDNA using oTO1212-oTO1430 and assembled into the vector amplified from pTO223 using oTO1431-oTO1432. The repair cassette was amplified using oTO945-oTO946 and transformed into CauTO261 to generate CauTO438.

605 **pTO280:** The *SCF1* complementation vector was amplified from pTO223 using oTO1159-oTO1160, which incorporate a 1x FLAG tag at the A-B Domain junction. The resultant product was assembled in a single fragment Gibson assembly and used as template for site-directed mutagenesis.

610 **pTO281/CauTO433:** The entire pTO280 vector was amplified in two overlapping fragments using overlapping backbone-specific primers oTO1427 and oTO1428 paired with oTO1418 and oTO1417, respectively. oTO1418 and oTO1417 contain overlapping sequence with the point mutations instantiated. The repair cassette was amplified using oTO945-oTO946 and transformed into CauTO261 to generate CauTO433.

615 **pTO282/CauTO434:** The entire pTO280 vector was amplified in two overlapping fragments using overlapping backbone-specific primers oTO1427 and oTO1428 paired with oTO1422 and oTO1421, respectively. oTO1422 and oTO1421 contain overlapping sequence with the point mutations instantiated. The repair cassette was amplified using oTO945-oTO946 and transformed into CauTO261 to generate CauTO434.

620 **pTO283/CauTO430:** The entire pTO280 vector was amplified in two overlapping fragments using overlapping backbone-specific primers oTO1427 and oTO1428 paired with oTO1426 and oTO1425, respectively. oTO1426 and oTO1425 contain overlapping sequence with the point mutations instantiated. The repair cassette was amplified using oTO945-oTO946 and transformed into CauTO261 to generate CauTO430.

625 **pTO268/CauTO432:** The N-terminal domain of *SCF1* was synthesized with the point mutations instantiated and cloned into the PCR product of pTO223 generated from oTO1159-591. The repair cassette was amplified using oTO945-oTO946 and transformed into CauTO261 to generate CauTO430.

630 **pTO292/CauTO453:** The entire pTO280 vector was amplified in two overlapping fragments using overlapping backbone-specific primers oTO1427 and oTO1428 paired with oTO1564 and oTO1563, respectively. oTO1563 and oTO1564 contain overlapping sequence with the point mutations instantiated. The repair cassette was amplified using oTO945-oTO946 and transformed into CauTO261 to generate CauTO453.

635 **pTO293/CauTO455:** The entire pTO280 vector was amplified in two overlapping fragments using overlapping backbone-specific primers oTO1427 and oTO1428 paired with oTO1566 and oTO1565, respectively. oTO1566 and oTO1565 contain overlapping sequence with the point mutations instantiated. The repair cassette was amplified using oTO945-oTO946 and transformed into CauTO261 to generate CauTO455.

C. auris Transformation

640 *C. auris* transformation was performed using a transient-Cas9 expression approach as described previously (52). Briefly, transformation repair cassettes were amplified from assembled plasmids. A Cas9 expression cassette was amplified from pTO135 using oTO143-oTO41. Cassettes for the expression of sgRNA targeting specific loci were amplified from pTO136 using overlap-extension PCR to change the gRNA sequence. All linear PCR products were purified using a Zymo DNA Clean & Concentrator kit (Cat no. D4034, Zymo Research) according to the manufacturer's instructions.

650 To prepare electro-competent cells, *C. auris* cells were incubated in liquid YPD at 30 °C overnight with gentle agitation. Cells were harvested by centrifugation and resuspended in TE buffer with 100 mM Lithium Acetate and incubated at 30 °C for 1 hr with constant shaking. DTT

655 was added to the cells at a final concentration of 25 mM before further incubating at 30 °C for 30 min. Cells were harvested by centrifugation at 4 °C before being washed once with ice-cold water and once with ice-cold 1 M Sorbitol. Harvested cells were resuspended in ice-cold 1M sorbitol and maintained on ice for immediate usage or aliquoted and stored at -80 °C for up to several months before transformation.

660 Electroporation was performed by adding 45 µL competent cells to a pre-chilled 2 mm-gap electro-cuvette along with 500-1000 ng each of the PCR-amplified Cas9, sgRNA, and repair cassettes. Cells were electroporated using a Bio-Rad MicroPulser Electroporator according to the pre-defined *P. pastoris* (PIC) protocol (2.0 kV, 1 pulse). Electroporated cells were recovered in 1 M Sorbitol then resuspended in YPD and allowed 2 hrs of outgrowth at 30 °C with constant rotation. Outgrown cells were spread-plated on selective media. For repair cassettes encoding the *NAT* marker, cells were selected on YPD + 200 µg/mL nourseothricin and incubated at 30 °C for 2-3 days. For repair cassettes encoding the *NEO* marker, cells were selected on YPD + 1 mg/mL G418 and incubated at 23 °C for 4 days or YPD + 1 mg/mL G418 + 1 mg/mL Molybdate (53) and incubated at 30 °C for 2-3 days. Transformant colonies were passaged to isolation and correct incorporation of the repair cassette was confirmed for each by colony PCR using Phire Plant Direct PCR Master Mix (F160; Thermo Fisher Scientific) according to the manufacturer's instructions. Each mutant was confirmed by at least three independent PCR reactions with distinct primer sets specific to the mutation site and compared to parental strains. Deletion mutants were confirmed with gene-specific primers based on absence of amplification from the ORF and integration of the repair cassette at the genetic locus. For mutants encoding site-directed mutations, genomic DNA was isolated and the entire genetic locus spanning the gene and sequence surrounding the integration junctions was PCR-amplified and sequenced to confirm the site-directed mutations were intact and no unintended mutations were present at the locus.

670
675
680 *C. haemulonii* Transformation

C. haemulonii transformation was performed similarly to *C. auris* transformation, except the outgrowth was extended to 5 hrs and transformants were selected on YPD + 50 µg/mL nourseothricin at 30 °C for 3 days.

685 *Agrobacterium tumefaciens*-Mediated Transformation (AtMT)

690 AtMT was performed as described previously (52). Briefly, *A. tumefaciens* strain pTO131 (EHA 105 harboring pTO128) was grown overnight at 30 °C in liquid LB media containing kanamycin. *A. tumefaciens* cells were harvested by centrifugation, washed once with sterile water, then resuspended at a final OD₆₀₀ of 0.15 in liquid Induction Medium (IM) supplemented with 100 µM acetosyringone 3',5'-dimethoxy-4-hydroxyacetophenone (AS) and incubated at room temperature for 6 hrs with constant agitation. Recipient *C. auris* AR0382 cells were grown overnight at 30 °C in YPD and harvested by centrifugation then resuspended in sterile water at a final OD₆₀₀ of 1.0. Prepared *A. tumefaciens* and *C. auris* cells were combined at equal volumes and the mixed culture was incubated on solid IM Agar supplemented with AS at 23 °C for 4 days. Cells were harvested into liquid YPD. The resulting suspension was washed three times by low-speed centrifugation to separate fungal cells from bacterial cells and aliquots of the washed culture were spread-plated on YPD + 200 µg/mL nourseothricin + 200 µg/mL cefotaxime. Plates were incubated at 30 °C for 2 days. Transformant colonies were manually arrayed into 96 well plates and grown overnight in YPD at 30 °C. Each well was overlayed with 50% glycerol and arrayed plates were frozen and stored at -80 °C.

AtMT Transgene Insertion Site Identification

705 Identification of transgene insertion sites was performed as described previously (52). Briefly, genomic DNA was isolated from mutants of interest and sequenced by Illumina sequencing. Library preparation, quality control, and Whole Genome Sequencing were performed by SeqCenter (Pittsburg, PA, USA). Library preparation was performed based on the Illumina Nextera kit and sequencing performed on the Nextseq 550 platform to generate 150 bp paired-end sequencing reads. Sequencing data was analyzed using the Galaxy web platform public server at *usegalaxy.org* (54). Read quality was assessed using FastQC and reads were trimmed using Trimmomatic (55) with a Phred quality cutoff of 20. Processed reads were then mapped to a linearized reference sequence of pTO128 (pPZP-Nat) using the Burrows-Wheeler Aligner with maximum exact matches (BWA-MEM) (56) configured with minimum seed length = 50 and band width = 2. Soft clipped read sequence corresponding to genomic DNA neighboring the T-DNA integration junction was extracted from the aligned BAM file using the extractSoftClipped script from SE-MEI (<https://github.com/dpryan79/SE-MEI>). The resulting sequences were mapped back to the *C. auris* B8441 reference assembly (NCBI GCA_002759435.2) using BWA-MEM with the default configuration to identify integration sites. T-DNA integration loci were confirmed for each sequenced mutant with Sanger sequencing.

RNA Extraction

725 RNA extraction was performed using a formamide extraction method (57). Briefly, cultured cells were harvested by centrifugation and all media was removed. Dry cell pellets were frozen on dry ice and stored at -80 °C before processing. To extract RNA, cell pellets were thawed at room temperature and resuspended in 100 µL FE Buffer (98% formamide, 0.01M EDTA). 50 µL of 500 µm RNase-free glass beads was added to this suspension and the mixture was homogenized for 30 sec 3 times using a BioSpec Mini-Beadbeater-16 (Biospec Products Inc., Bartlesville, OK, USA). The resulting cell lysate was clarified by centrifugation to remove cell debris. The supernatant was collected as the crude RNA extract. The crude extract was purified using a Qiagen RNeasy mini kit (ref 74104, Qiagen) according to the manufacturer's instructions. Samples were DNase treated with Invitrogen DNase (RNase free) (Qiagen, cat no. 79254). The integrity and purity of the extracted RNA was confirmed via Nanodrop and agarose gel electrophoresis prior to downstream applications.

RT-qPCR

740 Purified RNA from cells cultured overnight in YPD at 30 °C was used to generate cDNA using the iScript cDNA synthesis kit (cat. 1708890, Bio-Rad Laboratories, Inc., Hercules, CA, USA) according to the manufacturer's instructions. Primers specific to target genes were designed using NCBI primer blast (58) with the *C. auris* B8441 assembly (NCBI GCA_002759435.2) or the *C. haemulonii* B11899 assembly (NCBI GCA_002926055.1) as a reference. Prepared cDNA was used as a template in qPCR reactions with the Power-Up SYBR Green Master Mix (cat. A25741, ThermoFisher Scientific, Waltham, MA, USA) according to the manufacturer's specifications. Cycling was performed using a Bio-Rad CFX Opus 384 Real Time PCR System. For *C. auris*, amplification of *ACT1* was measured using primers oTO359-oTO360, of *SCF1* using primers oTO1251-oTO1252, and of *IFF4109* using primers oTO615-oTO616. For *C. haemulonii*, amplification of *ACT1* was measured using primers oTO1253-oTO1254 and amplification of *SCF1* was measured using primers oTO1229-oTO1230.

RNA-Seq

Purified RNA from cells cultured to mid-exponential phase in YPD at 30 °C was sequenced by SeqCenter (Pittsburgh, PA, USA). Library preparation was performed using the Stranded total RNA Prep Ligation with Ribo-Zero Plus kit (Illumina, San Diego, CA, USA) and 10bp IDT for Illumina indices. Sequencing was performed using the NextSeq2000 platform to generate 2 x 50 bp reads. Sequencing data was analyzed using the Galaxy web platform public server at usegalaxy.org (54). Read quality was assessed using FastQC and reads were trimmed for quality using Cutadapt (59) with a Phred cutoff score of 20. Reads were then mapped to the *C. auris* B8441 reference assembly (NCBI GCA_002759435.2) using RNA Star (60) with the default parameters. Mapped reads were quantified using featureCounts (61) and differential expression was assessed using DESeq2 (62). Genes with a fold change greater than 2 times upregulated or downregulated and an adjusted p-value less than 0.05 were considered statistically significant.

Dispersed Surface Flow Cytometry Adhesion Assay

Adhesion to polystyrene was assessed using a previously established flow cytometric assay to measure the proportion of a population of cells able to attach to dispersed polystyrene surfaces in one hour (28). Cells from overnight culture were suspended in YPD containing green fluorescent polystyrene microspheres (1 µm, F-8823, Molecular Probes) at a ratio of 10 microspheres to 1 cell. For experiments involving additives, cells and microspheres were suspended in YPD containing the appropriate concentration of additive (NaCl or amino acids) and adjusted to neutral pH. This mixture was incubated with continuous inversion at 25 revolutions/min for 1 hour at room temperature. Cells were fixed with 4% formaldehyde for 10 minutes at room temperature, then washed and resuspended in PBS for flow cytometric analysis. Samples were analyzed using an LSRFortessa Flow Cytometer (BD Biosciences, NJ, USA) using a standard filter (FITC, 530/30). Acquisition settings were defined using the green fluorescent polystyrene microsphere samples to adjust the voltage of the fluorescent channel to the fourth logarithmic decade. Gating was performed as described in Fig S1. FSC was used to gate cells from unattached microspheres. Data was collected for 10,000 gated events, which represented two distinct fluorescent populations. The percentage of cells with microspheres attached was determined by assessing the ratio of fluorescent to total events.

High Throughput Adhesion Assay

An automated imaging-based assay was used for high throughput adhesion measurements. A total of 2,560 insertional mutants in the AR0382 strain background were arrayed and individually assayed in 96-well plates. Arrayed mutants were cultured from glycerol stocks on solid YPD agar at 30 °C. The resulting colonies were used to seed 200 µL YPD cultures in 96 well plates and grown overnight at 30 °C. For the adhesion assay, cells from each well were transferred into 100 µL YPD in a CellCarrier-96 Ultra Microplate with an optical cyclic olefin polymer surface (cat #NC1463153, Perkin Elmer, Waltham, MA, USA) using a 96-well microplate replicator (RePad 96 long pin, REP-001, Singer Instruments, United Kingdom). A single layer of visually distinct cells on the well surface were transferred. Each microplate contained 80 individual wells of mutants and 8 wells each of AR0382 and AR0387 as high adhesion and low adhesion controls, respectively. After adding cells, the plates were centrifuged at 210 x g for 1 minute to settle the cells. Cells were incubated on the surface of the well for 1 hr at room temperature to allow for attachment. Unattached cells were removed by washing each well 3 times with 100 µL PBS and using a vacuum aspirator with 8 channel manifold (BrandTech QuickSip aspirator) to remove media between each wash. Each well was imaged in

800 brightfield using a Yokogawa CellVoyager CQ1 automated microscope before and after washing. Four fields containing an average of approximately 1,000 cells/field were captured in defined positions such that the same four regions were imaged for each well before and after washing. Pre-processing of images was performed in Fiji ImageJ software (version 1.52) (63) using a custom macro that segmented cells in the brightfield images using edge detection and generated a binary mask from the segmented cells. The pre-processed images were quantified using CellProfiler software (version 3.1.9) (64) to generate a cell count for each captured field. A ratio of adhesive cells was calculated by dividing the count of the attached cells remaining after washing by the count of the input cells for each captured field.

805 The dynamic range of the assay was determined using a plate containing 48 wells of AR0382 and 48 wells of AR0387 as high and low adhesion controls, respectively. To determine the degree of separation between the two controls, the z-factor for the assay was calculated based on an established formula (65). Similarly, a z-factor was calculated based on the control wells for each mutant plate tested. The average z-factor for the control-only condition was 0.7167, indicating sufficient separation to detect differences between high and low adhesive strains, where an acceptance criteria of $0.5 < \text{z-factor} < 1.0$ was established for each mutant plate based on the control wells for that plate.

810 A z-score was assessed for each mutant by subtracting the proportion of adhesive cells from the average proportion of adhesive cells amongst all the mutants and dividing by the standard deviation amongst all the mutants. Mutants with a z-score more negative than -3 were considered to have significantly reduced adhesion.

Flocculation Assay

815 Cells were cultured overnight in YPD at 30 °C. Cultures were vortexed to suspension for 10 sec at max speed, then placed upright at room temperature and allowed to settle for 20 min. Immediately after vortexing and at specified timepoints, a 20 µL aliquot was gently removed from the top of the culture and diluted to optical range in a 96 well plate. OD₆₀₀ was measured for each removed aliquot using a BioTek 800 TS absorbance reader. Flocculation activity was calculated as the percent reduction in OD₆₀₀ in aliquots at each timepoint compared to the initial reading.

Immunofluorescence Microscopy and Flow Cytometry

820 Wild type and $\Delta scf1 + SCF1-FLAG$ cells were cultured overnight in YPD at 30 °C then harvested by centrifugation and washed in PBS. The cells were fixed with 4% formaldehyde for 10 min at room temperature, then washed and resuspended in PBS. Once fixed, the cells were blocked in 2% BSA for 60 min. The cells were then pelleted and resuspended in 0.1% BSA containing a 1:500 dilution of primary antibody (Rabbit α-FLAG Polyclonal, Sigma F7425) and incubated at room temperature for 3 hrs. The primary antibody was removed, and the cells were resuspended in 0.1% BSA containing a 1:500 dilution of secondary antibody (Goat α-Rabbit IgG, Alexafluor 594, Invitrogen A11037) and incubated at room temperature for 45 min, protected from light. The cells were washed three times in PBS with 0.1% Tween-20 and resuspended in PBS. Microscopy was performed using a Bioteck Lionheart FX automated microscope using 100X oil objective (Olympus 1.4NA) and the TexasRed imaging filter cube and LED. Flow Cytometry was performed using an LSRII Fortessa Flow Cytometer (BD Biosciences, NJ, USA)

845 using a standard filter (PE-Texas Red, 610/20). Data was collected for 50,000 events. Median fluorescence intensity was calculated using FlowJo™ v10.8.2 Software (BD Life Sciences).

Homology Search and Structural Prediction

850 The genomic and protein sequence for *SCF1* (B9J08_001458) was retrieved from the B8441 reference assembly (NCBI GCA_002759435.2). Protein domain organization was determined based on automatic annotations from the UniProt database. To search for *SCF1* homologs, either the entire sequence or the N-terminal domain sequence were subjected to a BLAST search with an E value cutoff of 0.05. Significant hits that only exhibited homology in low complexity, repetitive regions were disregarded. The only remaining hits found were in *C. auris* or *C. haemulonii* genomes. Synteny of the *SCF1* locus was evaluated using the annotations available through the FungiDB database (66) and Candida Gene Order Browser database (67).

855 The N-terminal domain was modeled using AlphaFold2 through the ColabFold platform (68). The *FLO11*-like Fibronectin-III fold was annotated through UniProt. Searching with Foldseek (69) returned proteins across the domains of life containing Fibronectin-III folds, including *FLO11* homologs. To assess the similarity to *FLO11*, *SCF1* and *FLO11* sequence and N-terminal sequence were cross-blasted against the *S. cerevisiae* or *C. auris* genome, respectively, which returned no significant homology with an E value cutoff of 0.05. The N-terminal domains were aligned to determine percent identity and to compare the positions of functionally critical aromatic bands from Flo11 to the Scf1 sequence.

Microbial Attachment to Hydrocarbons (MATH) Assay

860 Cell surface hydrophobicity was determined using the microbial adhesion to hydrocarbon (MATH) assay (70), which measures the fraction of cells sequestered out of aqueous suspension by pure hydrocarbon. Overnight cultures were harvested by centrifugation and washed three times in PBS. The cells were standardized to an OD₆₀₀ of 0.4 in PBS using a Bio Tek 800 TS microplate reader. An aliquot of the cell suspension was reserved for an initial OD₆₀₀ reading (A0). 1200 µL of each cell suspension in PBS was transferred into clean, unused borosilicate glass test tubes with a 10 mm diameter. 200 µL n-hexadecane (Sigma-Aldrich, cat no: H6703) was gently overlaid atop the culture suspension in the test tube. The tubes were allowed to rest for 10 minutes at room temperature, then capped and vortexed at max speed for 1 min to mix the hydrocarbon and aqueous phases. The tubes were left for 15 minutes at room temperature to allow for separation of phases, after which an aliquot of the lower aqueous layer was taken for the final OD₆₀₀ reading (A1). The proportion of sequestered cells were calculated by dividing the final OD₆₀₀ reading (A1) by the initial reading (A0) according to the formula: [1 – (A1/A0)] * 100%.

Plasma Etched Polystyrene Adhesion

865 Adhesion of *C. auris* cells to hydrophobic and hydrophilic substrates was modeled using untreated or surface-modified polystyrene multi-well plates (Nest Biotechnology Co., cat. 701311), which were considered to be hydrophobic as untreated (71). To assess adhesion to a hydrophilic substrate, the surface hydrophobicity of the polystyrene was modified by the addition of free radicals using vacuum plasma treatment. The plate was placed without the lid in a PE-25 plasma cleaner (Plasma Etch Inc, Nevada, USA) and treated for 90 seconds at 400W 50 kHz with 200 mtorr / 27 Pa vacuum pressure. The plate was tested to be fully water-wettable by visual examination of a droplet spreading on the surface and compared to an untreated (hydrophobic) polystyrene plate. *C. auris* cells were cultured overnight in YPD at 30 °C and

added to either the hydrophobic or hydrophilic polystyrene plates. Cells were centrifuged at 210 x g for 1 min to gently settle a single layer of cells on the polystyrene surface. Plates were incubated for 1 hr at room temperature to allow for attachment. For each well, images of four fields in defined positions were taken in brightfield using a BioTek Lionheart FX automated microscope. Unattached cells were removed by washing 3 times with PBS, and fields in the same defined positions were imaged after washing. Cell counts for each field were determined using image analysis software as described above. The percentage of adherent cells was calculated by dividing the count of the attached cells remaining after washing by the total number of the cells input for each captured field.

Peptide-Microparticle Binding

13-amino acid peptides corresponding to WT Scf1 residues 50-62 or the same sequence with H52A H53A R54A R55A mutations were synthesized with N-terminal tetramethylrhodamine (TMR) labels (Genscript, NJ, USA). Peptide purity was confirmed to be ~95% or greater by HPLC. Peptides were dissolved in PBS, pH 7.4 (Ref. 10010-023, Gibco). For microsphere binding measurements, peptides were mixed with polystyrene microspheres (1 μ m, F-8823, Molecular Probes) or phosphatidylcholine (PC) lipid microparticles (3 μ m, P-B1PC, Echelon Biosciences) suspended in YPD and vortexed at max speed for 1 minute. Peptide binding was assessed using a Biotek Lionheart FX automated microscope with the TRITC imaging filter cube and LED. Mean fluorescence intensity of individual particles was measured and corrected for background fluorescence using Gen5 software (version 3.12).

Whole Cell Lipid Particle Binding

Cells from overnight culture were suspended in YPD containing green fluorescent PC lipid microparticles (3 μ m, P-B1PC, Echelon Biosciences) at a ratio of 1 microparticle to 10 cells. This mixture was incubated with continuous inversion at 25 revolutions/min for 1 hour at room temperature. Aliquots were dispensed into 96-well plates and centrifuged at 210 x g for 1 min to settle cells and lipid particles before imaging using a Biotek Lionheart FX automated microscope with the GFP imaging filter cube and LED. Lipid particles were segmented from the image based on green fluorescence and the fraction of bound particles was calculated by dividing the number of particles colocalizing with cells by the total number of lipid particles.

In vitro Biofilm Formation

Cells were cultured overnight in YPD at 30 °C and resuspended in RPMI-1640 media. Each strain was standardized to a starting OD₆₀₀ of 0.5 in RPMI and seeded in 200 μ L in 96-well plates with a virgin polystyrene surface. The seeded plates were sealed with a breathable membrane and incubated for 90 min at 37 °C with shaking at 250 rpm to allow for attachment. After this initial incubation, the media was aspirated and each well was washed with 200 μ L PBS before replacing the liquid in each well with fresh RPMI-1640 media. The plates were sealed and biofilms were allowed to form for 24 hrs at 37 °C with constant orbital shaking at 250 rpm. After 24 hrs, each well was washed three times with 200 μ L PBS. To quantify the oxidative activity of the viable biofilms, a colorimetric XTT reduction assay was performed (72). A 0.5 mg/mL XTT (XTT sodium salt, cat #AAJ61726MD, Thermo Scientific) solution in PBS was combined with a 0.32 mg/mL PMS (Phenazine Methosulfate, cat #10955, MP Biomedicals) solution in water at a 9:1 XTT:PMS ratio and 100 μ L was added to each biofilm. The plate was incubated at 37 °C for 30 min before removing the media to a clean 96 well plate and measuring the OD₄₉₂. To image biofilms, the biofilms were fixed with 4% formaldehyde for 10 minutes at room temperature then washed two times with 200 μ L PBS. The fixed biofilms were stained with calcofluor white (cat

#18909, Sigma-Aldrich) for 10 minutes then washed three times with 200 μ L PBS. Stained biofilms were imaged in Z-stacks using a Biotek Lionheart FX automated microscope at 400x magnification with the DAPI imaging filter cube and LED. Maximum intensity projections were generated using Gen5 software (version 3.12).

945

Rat Catheter Biofilm Formation

In vivo biofilm testing was performed with a rat external jugular venous catheter model as previously described (73). Briefly, a 10^6 cells/ml inoculum for each strain was allowed to grow on an internal jugular catheter placed in specific-pathogen-free Sprague–Dawley rats (16-week old, 400 g) for 24 h. After this period, biofilm formation on the intraluminal surface of the catheters was observed by scanning electron microscopy. SEM images were acquired on a ZEISS Gemini 450 scanning electron microscope using an accelerating voltage of 3.0 kV, a working distance of 6 mm, an Everhart-Thornley SE2 detector with optically coupled photomultiplier, and the ZEISS SmartSEM (v. 6.05) software. Procedures were approved by the Institutional Animal Care and Use Committee at the University of Wisconsin, Madison (protocol MV1947).

950

Ex vivo Human Skin Bioburden

Human skin samples were collected from patients through an IRB-exempt protocol (74). Full-thickness excised skin samples were placed in 12-well plates containing 3 mL of Dulbecco's Modified Eagle Medium (DMEM) (Lonza, Walkersville, MD, USA), supplemented with 10% FBS (Atlanta Biologicals, Lawrenceville, GA, USA), penicillin (1000 U/mL), and streptomycin (1 mg/mL) (74, 75). After 24 h, samples were washed with DPBS and moved to semi-solid media (6:4 ratio of 1% agarose (BIO-RAD, Hercules, CA, USA) in DPBS and DMEM with 10% FBS). Paraffin wax was applied as a barrier between the epidermal surface and the semi-solid media. *Candida* spp. (10 μ L at 10^7 cells/mL) were applied to the skin surface. Skin samples were incubated at 37 °C for 24 h, rinsed, and processed for viable burden determination or microscopy. For microscopic analysis, skin samples were fixed overnight (4% formaldehyde, 1% glutaraldehyde, in sodium phosphate buffer), washed with sodium phosphate buffer, stained with 1% osmium tetroxide in DPBS, and dehydrated by ethanol rinsing. Samples were then dried using three changes of Hexamethyldisiazane (1 h each) followed by air desiccation for 48 h. Samples were mounted on aluminum stubs with silver paint applied at the interface. Samples were then platinum sputter coated and imaged by scanning electron microscopy (Zeiss Gemini 450, 3 kV).

960

965

970

975

Intravenous Murine Infection

Overnight cultures of *C. auris* were pelleted by centrifugation at 4000 rpm for 10 min at 4 °C, followed by washing three times with 1X Dulbecco's Phosphate Buffer Saline (DPBS). The yeast cells were finally suspended in 1X DPBS and counted by using a hemocytometer. The yeast cell densities were adjusted at 2.5×10^8 cells/ml (5×10^7 cells/0.2 ml) using 1X DPBS. Infection was performed using an immunosuppressed mouse model of *C. auris* infection with hematogenous dissemination to assess the virulence of various *C. auris* strains *in vivo*. Briefly, outbred ICR CD-1 mice, aged 4-6 weeks (n=10+1/group), were subjected to immunosuppression by intraperitoneal (i.p.) injection of 200 mg/kg cyclophosphamide and subcutaneous injection of 250 mg/kg cortisone acetate on day -2 prior to infection. To prevent bacterial superinfection in the immunosuppressed mice, enrofloxacin was added to the drinking water at a concentration of 50 μ g/mL on the day of immunosuppression and continued for two weeks. The mice were then infected with various *C. auris* strains via tail vein injection, using the inoculum of 5×10^7 yeast

990 cells in 0.2 ml per mouse. The survival of the infected mice was monitored for a duration of 21 days. For histopathological examination of the infected mice, an additional mouse was included in each group. On day 7 post-infection, one mouse from each group was euthanized, and their kidneys and heart were collected for further analysis. The harvested organs were fixed in 10% zinc-buffered formalin, embedded in paraffin, and then sectioned. To visualize the tissue, Pacific Acid Schiff (PAS) stain was applied to the sections. The stained tissue sections were then imaged using Olympus microscopy.

Epicutaneous Murine Infection

995 The murine epicutaneous infection was performed as previously described with modifications (76). Infection was performed using C57BL/6J mice at 7 weeks of age (Jackson Laboratories). Mouse dorsal hairs were shaved one day before infection. For infection, *C. auris* strains were cultured overnight at 30 °C, washed once with PBS, and resuspended at a concentration of 1×10^9 cells/ml in PBS using a hemocytometer. 2×10^8 cells of *C. auris* were placed on a patch of sterile gauze and attached to the shaved skin of individual mice with a transparent occlusive plastic dressing (Tegaderm; 3M). The actual inoculum of each *C. auris* culture used for infection was also determined by colony-forming units (CFUs) on YPD+ampicillin + gentamycin plates. Mice were sacrificed after being exposed to *C. auris* for 2 days through the patch. Dorsal skin tissue underneath the gauze was harvested, weighed, and digested with 0.25 mg/ml liberase in 500 ul PBS for 1 hour and 45 minutes at 37 °C and 5% CO₂. Digested dorsal skin tissue was homogenized with a bead beater for 30 seconds x 4 times. The supernatant of each homogenized sample was plated on YPD + ampicillin + gentamycin plates to determine the CFUs recovered from each mouse. The number of CFU was determined after 48 h of incubation at 30 °C. The actual fungal burden for each mouse was determined by normalizing the CFUs recovered from each mouse by the weight of the recovered dorsal skin tissue and actual delivered inoculum.

Statistics and Reproducibility

1000 Statistical analyses were performed using R statistical software (version 4.0.3) using the DescTools package (version 0.99.49) for ANOVA and the survminer package (version 0.4.9) for survival analysis. Unless otherwise specified, experiments were performed in at least three independent biological replicates and data are presented as means ± standard error of means from biological replicates, with each point representing individual biological replicates. Microscopy and photography images are representative of at least 3 experiments with similar results. 1005 Statistically significant differences were calculated using student's t-test or one-way ANOVA with Tukey's or Dunnett's post hoc test for multiple comparisons. Correlation was measured using Pearson correlation. Differences in survival analysis were determined using a Mantel-Haenszel log-rank test with Benjamini-Hochberg correction. **p* ≤ 0.05; ***p* ≤ 0.01; ****p* ≤ 0.001; ns *p* > 0.05.

1010 Data are provided as a source data file (Data S1).

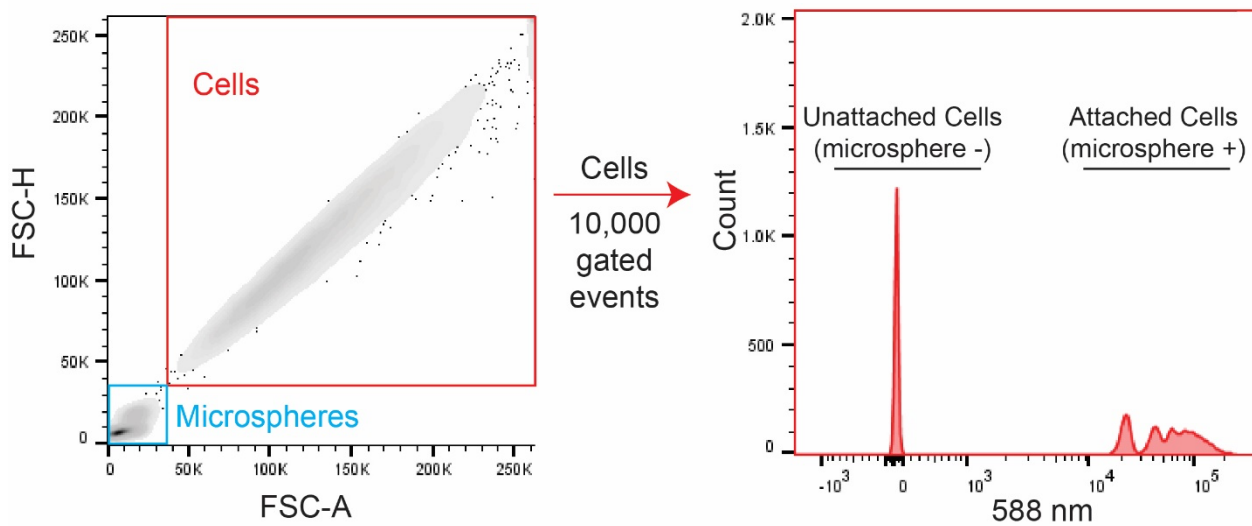


Fig. S1. Gating strategy for dispersed surface flow cytometry adhesion assay. Cells were gated from fluorescent microspheres using forward scatter. Ten-thousand gated events were collected for cells and divided into two populations using FITC fluorescence. Attached cells were identified by positive fluorescent signal. Attachment was expressed as the proportion of attached cells to the total population.

1035

1040

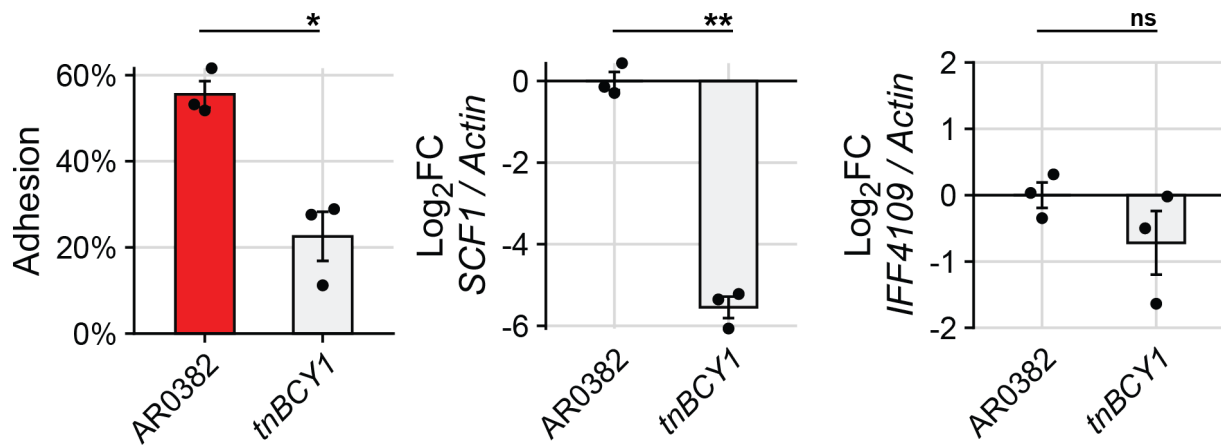


Fig. S2. A *BCY1* insertional mutant shows reduced adhesion associated with downregulation of *SCF1* but not *IFF4109*. Adhesion to polystyrene microspheres and transcript abundance compared to the parental AR0382 for *SCF1* and *IFF4109*. Statistical differences were assessed using student's t-test; *p ≤ 0.05; **p ≤ 0.01; ***p ≤ 0.001; ns: p > 0.05.

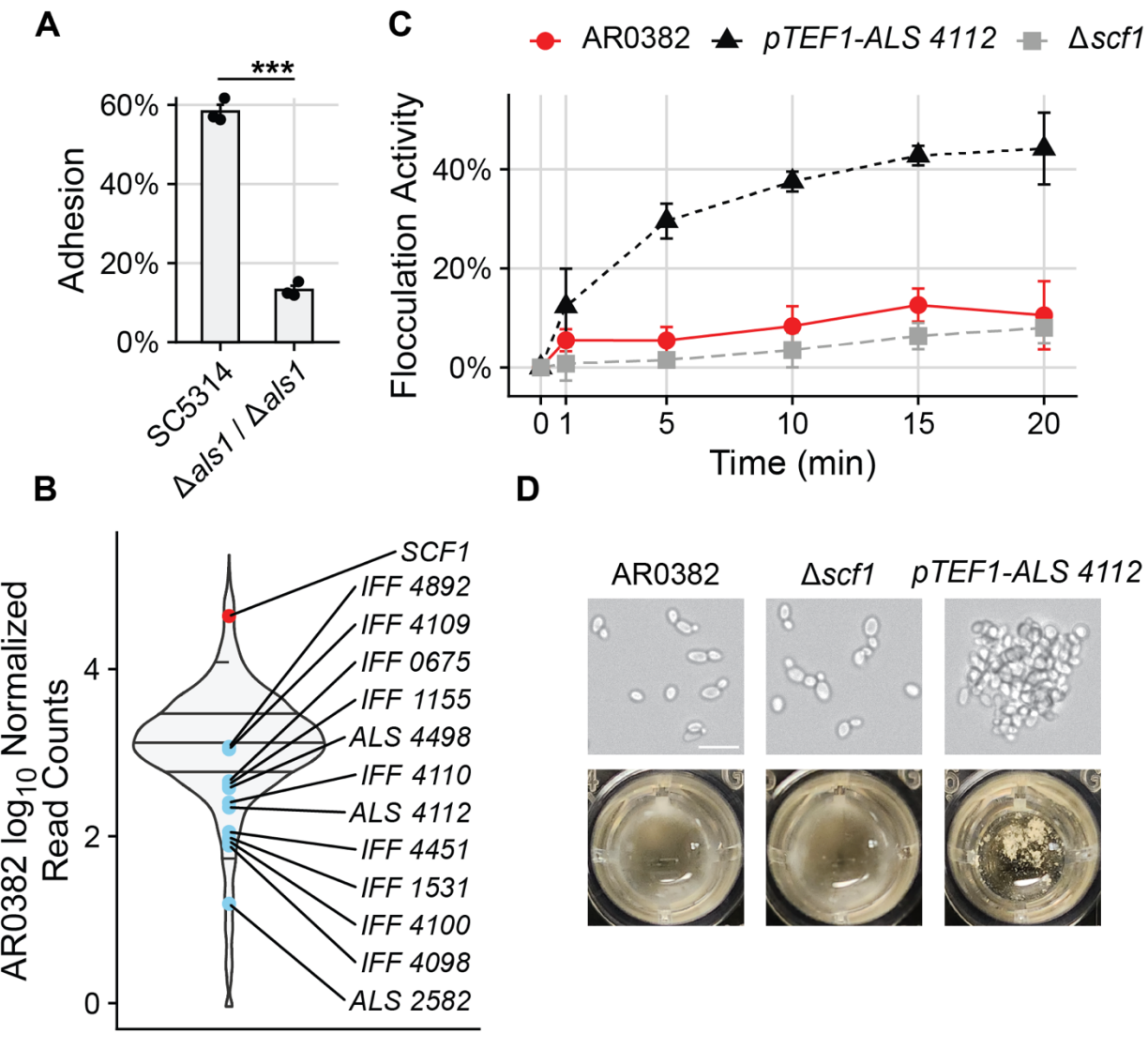


Fig. S3. Individual adhesin genes exhibit distinct phenotypes. (A) Adhesion to polystyrene microspheres measured for *C. albicans* SC5314 or a mutant lacking *ALS1*. Cells were grown in yeast phase in YPD at 30 °C. (B) DESeq-normalized read counts for all ORFs based on AR0382 RNA-seq. Read counts for adhesins are indicated. Horizontal lines mark the 5th, 25th, 50th, 75th, and 95th percentiles among all ORFs. (C) Flocculation activity measured over time for wild type AR0382 or mutants lacking *SCF1* or driving *ALS 4112* with the *C. auris* *TEF1* promoter. Data are mean ± SEM from three replicates. (D) Representative brightfield microscopy (top) and photographs of broth culture after 20 minutes of settling (bottom) for the strains assessed in (C). Scale bar = 10 µm. Statistical differences were assessed using student's t-test (A); *p ≤ 0.05; **p ≤ 0.01; ***p ≤ 0.001; ns: p > 0.05.

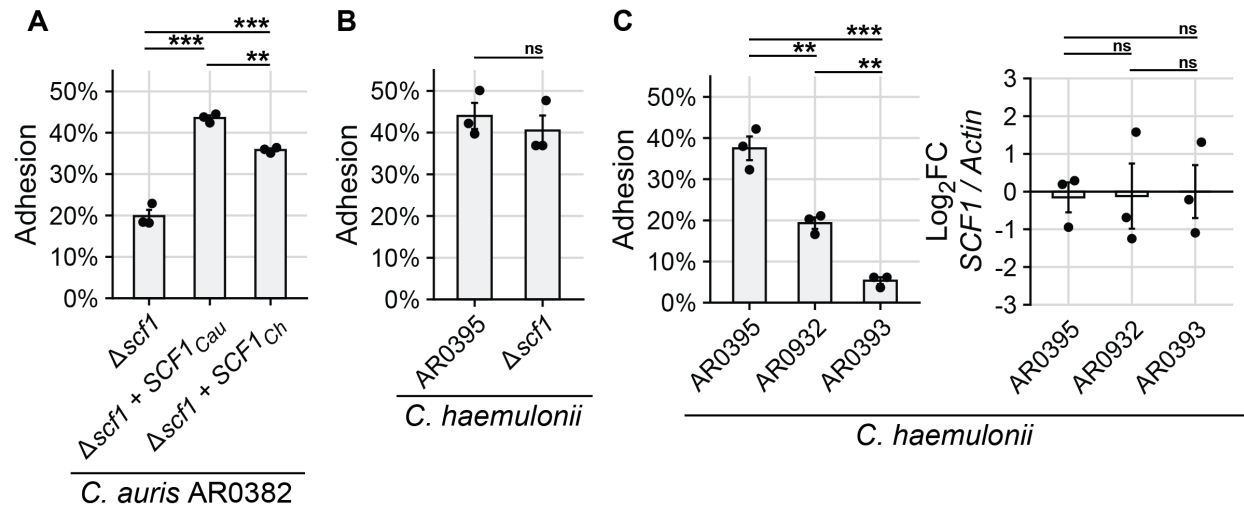


Fig. S4. *C. haemulonii* does not rely on *SCF1* for adhesion. (A) Adhesion of *C. auris* AR0382 $\Delta scf1$ mutant or the same mutant complemented with the *SCF1* allele from *C. auris* AR0382 or from *C. haemulonii* AR0395. (B) Adhesion of *C. haemulonii* AR0395 and a mutant lacking the putative *SCF1* homolog (CXQ85_003100). (C) Adhesion of three distinct *C. haemulonii* isolates and *SCF1* expression compared to AR0393. Statistical differences were assessed using student's t-test (B) or one-way ANOVA with Tukey's post-hoc test (A) and (C); *p ≤ 0.05; **p ≤ 0.01; ***p ≤ 0.001; ns: p > 0.05.

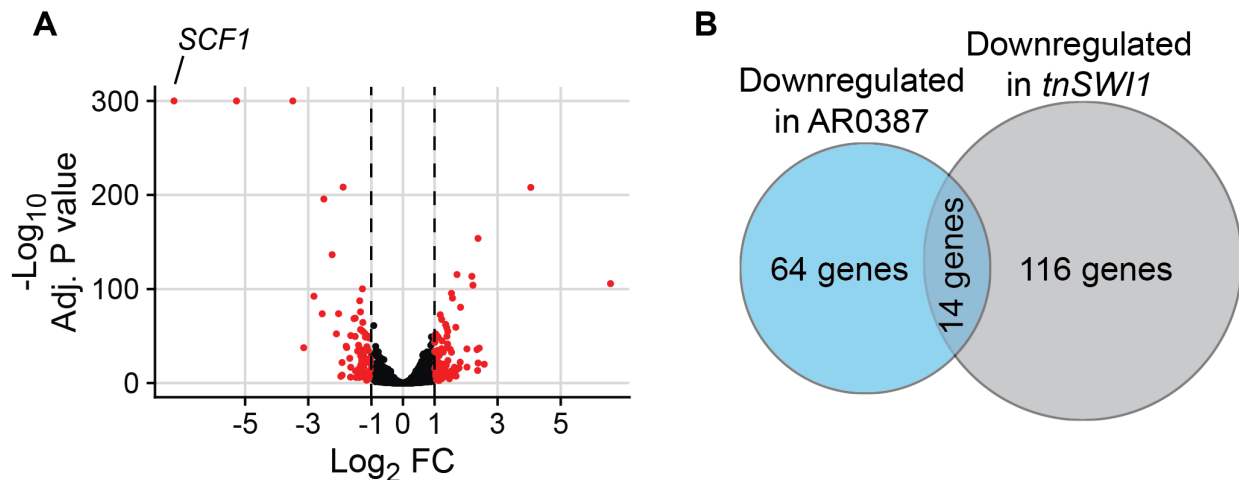


Fig. S5. *SCF1* is the most strongly dysregulated gene between AR0387 and AR0382. (A) Transcriptome of AR0387 compared to AR0382. Genes in red are significantly dysregulated in AR0387, with *SCF1* being the most strongly and most significantly downregulated gene. **(B)** Comparison of the downregulated transcriptome between two poorly adhesive strains compared to the strongly adhesive AR0382. The regulon of AR0387 and *tnSWI1* overlap by 14 genes.

1070

1075

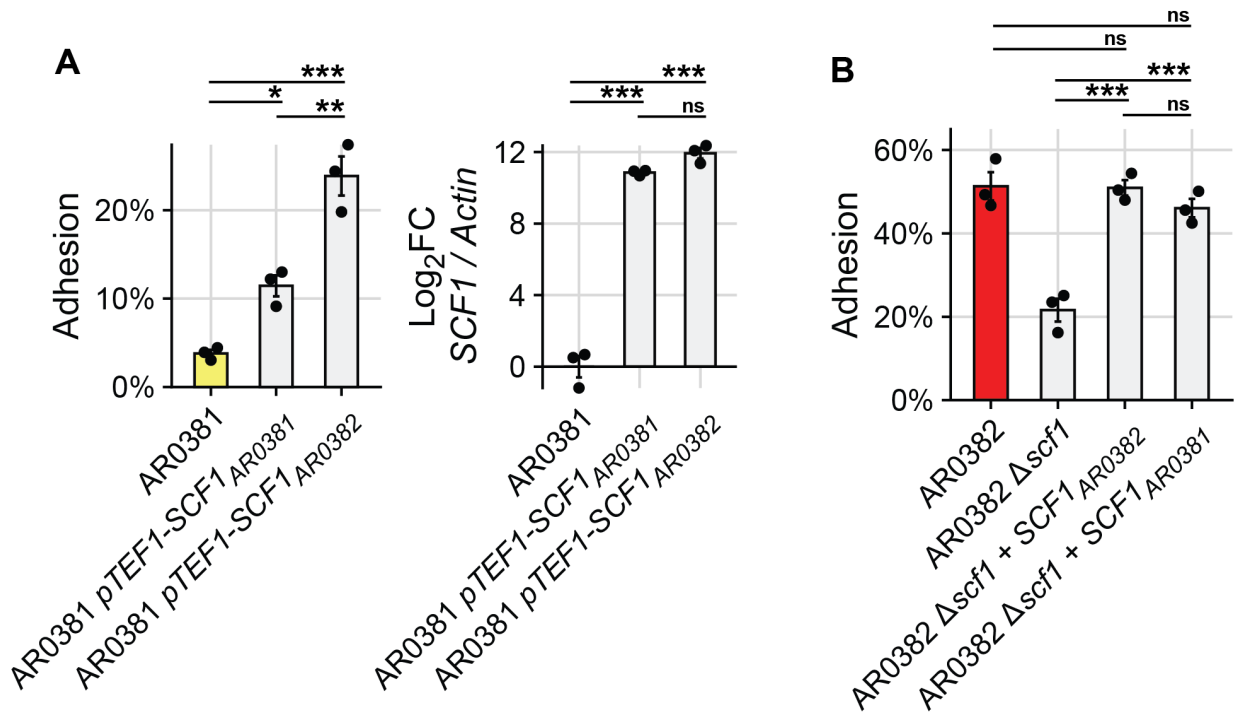


Fig. S6. Different *SCF1* alleles exhibit different magnitudes of attachment in a strain-dependent manner. (A) Overexpression of the AR0382 (Clade I) *SCF1* allele in AR0381 (Clade II) confers a stronger adhesive phenotype than overexpression of the endogenous AR0381 *SCF1* allele (left panel), despite similar transcript abundance (right panel). (B) The AR0382 $\Delta scf1$ attachment defect is fully rescued by complementation with the *SCF1* allele from either AR0382 or AR0381. Statistical differences were assessed using one-way ANOVA with Tukey's post-hoc test; *p ≤ 0.05; **p ≤ 0.01; ***p ≤ 0.001; ns: p > 0.05.

1080

1085

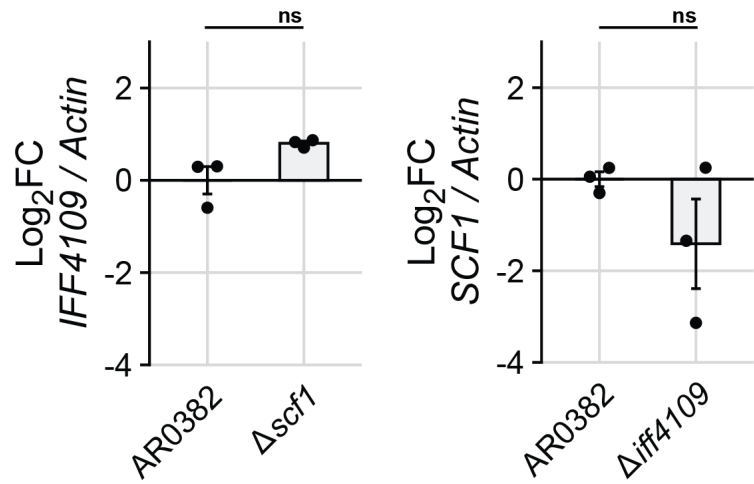


Fig. S7. Loss of either *SCF1* or *IFF4109* does not result in transcriptional dysregulation of the other. qPCR comparing transcript abundance for *IFF4109* or *SCF1* in strains lacking *SCF1* or *IFF4109* compared to the parental wild type. Statistical differences were assessed using student's t-test; *p ≤ 0.05; **p ≤ 0.01; ***p ≤ 0.001; ns: p > 0.05.

1090

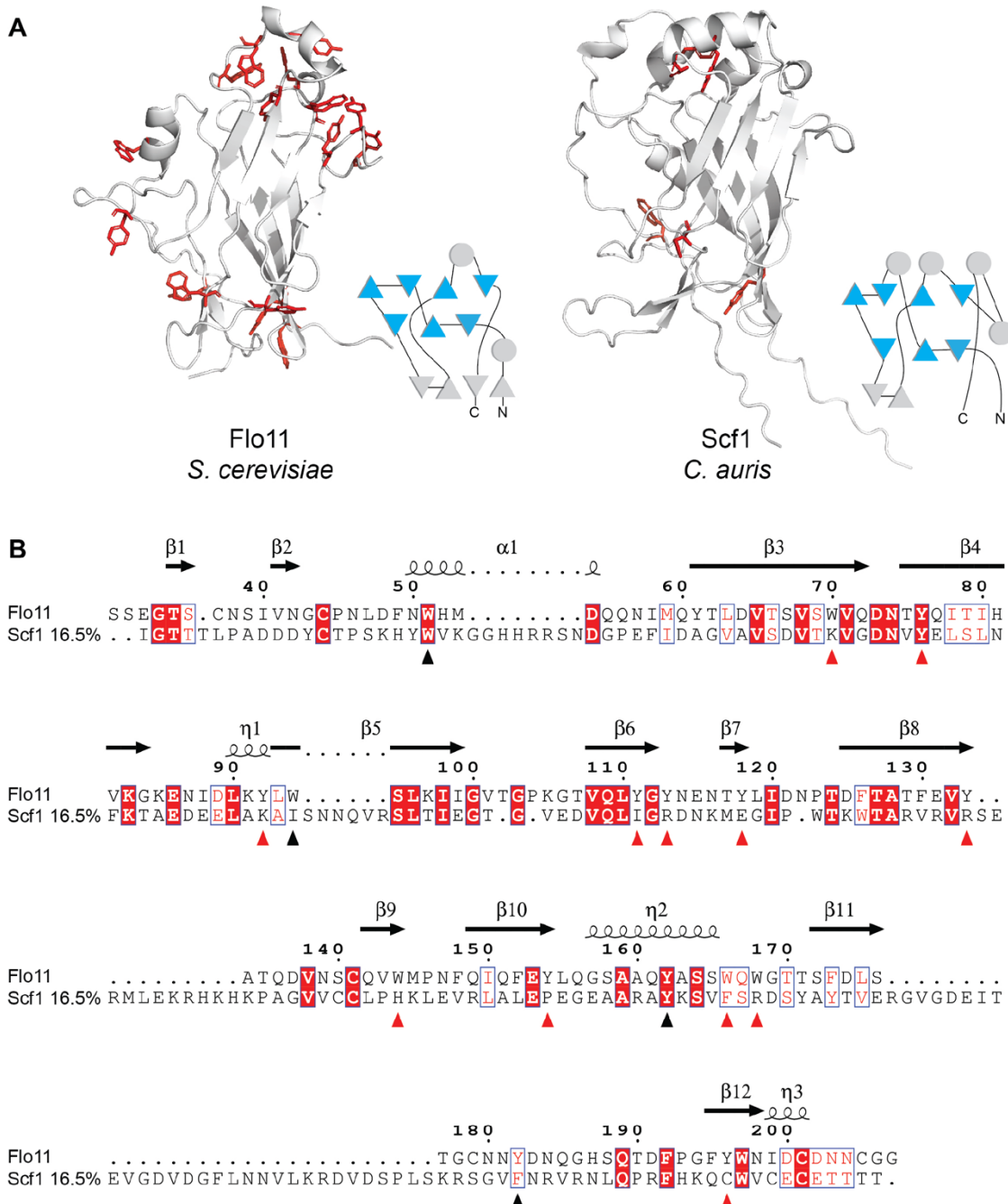
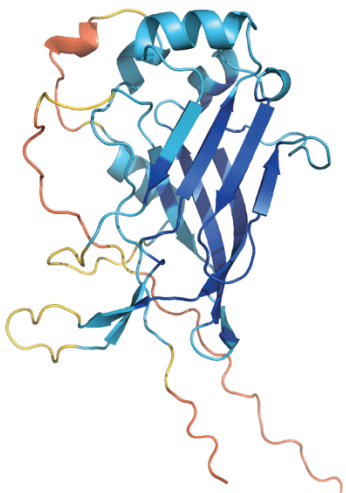
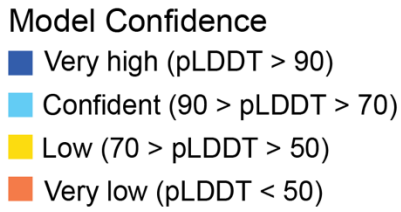


Fig. S8. The *SCF1* N-terminal domain contains a *FLO11*-like Fibronectin-type III fold but lacks conserved aromatic residues critical to Flo11 function. (A) N-terminal domain models for *S. cerevisiae* Flo11 (crystal structure) and *C. auris* Scf1 (AlphaFold2 predictive model) and membrane topology diagrams. Aromatic bands that are conserved and have functional roles in Flo11 homologues throughout *Ascomycota* are highlighted. The central Fibronectin-type III fold is highlighted in the topology diagrams. (B) Primary sequence alignment between *S. cerevisiae* Flo11 N-terminal domain and *C. auris* Scf1 N-terminal domain. Identical residues are boxed in red; similar residues are boxed in white. Inverted triangles indicate the positions of aromatic

1095

1100

residues that are conserved from *S. cerevisiae* to Flo11 homologues in other *Ascomycota* species. Red triangles indicate residues that have demonstrated functional roles in biofilm formation, invasive growth, or homotypic interactions.



1105

28	I G T T T L P A D D D Y C T P S K H Y W
48	V K G G H H R R S N D G P E F I D A G V
68	A V S D V T K V G D N V Y E L S L N F K
88	T A E D E E L A K A I S N N Q V R S L T
108	I E G T G V E D V Q L I G R D N K M E G
128	I P W T K W T A R V R V R S E R M L E K
148	R H K H K P A G V V C C L P H K L E V R
168	L A L E P E G E A A R A Y K S V F S R D
188	S Y A Y T V E R G V G D E I T E V G D V
208	D G F L N N V L K R D V D S P L S K R S
228	G V F N R V R N L Q P R F H K Q C W V C
248	E C E T T T T T

1110

Fig. S9. Predictive model confidence for the Scf1 N-terminal domain is substantially reduced outside of the Fibronectin-type III fold. N-terminal domain models for *C. auris* Scf1 (AlphaFold2 predictive model) and the domain sequence colored by per-residue pLDDT score. Cutoffs are set according to AlphaFold2 conventions. Numbers indicate amino acid position from the start codon.

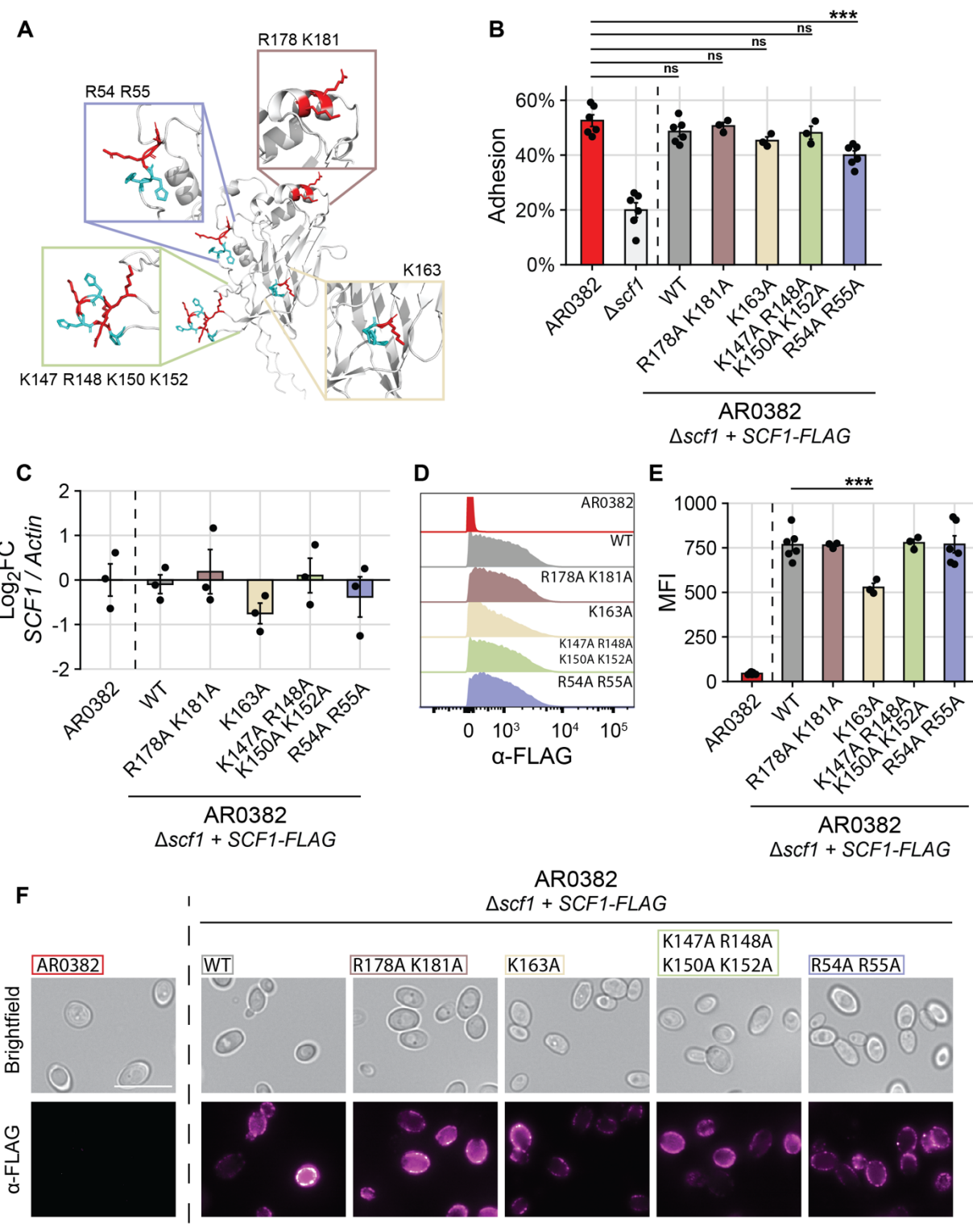


Fig. S10. Specific cationic residues are critical to the ability of Scf1 to mediate surface association. (A) Predictive model of the Scf1 N-terminal domain with hypothesized critical cationic residues highlighted in red and neighboring aromatic residues highlighted in blue. (B) Adhesion to polystyrene microspheres measured for wild type AR0382, a mutant lacking *SCF1*, or AR0382 $\Delta scf1 + SCF1-FLAG$ mutants encoding the wild type *SCF1* allele or alleles

containing the indicated mutations. **(C)** Relative *SCF1* transcript abundance by RT-qPCR compared to wild type AR0382 levels. No significant differences were identified. **(D)** Representative fluorescence intensity of strains labeled with α -FLAG antibody. Each plot represents 50,000 events captured by flow cytometry. **(E)** MFI quantification of replicates from labelled cells as in (B). **(E)** Brightfield and epifluorescent microscopy of cells labeled with α -FLAG antibody. Scale bar = 5 μm . Statistical differences were assessed using one-way ANOVA with Dunnett's post-hoc test using AR0382 as comparator (B), (C) or AR0382 $\Delta scf1 + SCF1$ -FLAG_{WT} as comparator (E); *p ≤ 0.05; **p ≤ 0.01; ***p ≤ 0.001; ns: p > 0.05.

1120

1125

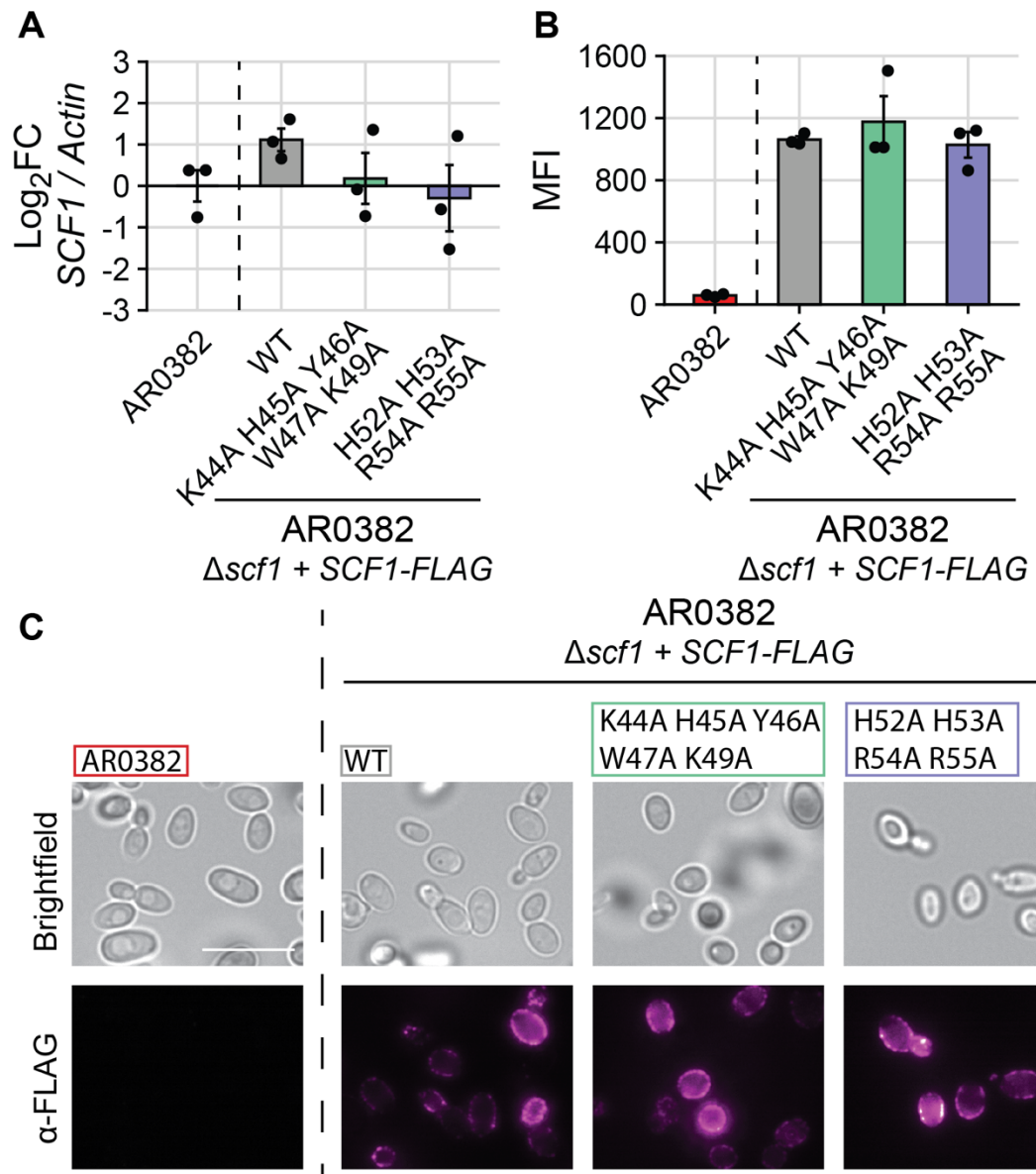


Fig. S11. Mutation of two adjacent cation-aromatic clusters does not impact *SCF1* expression or localization. Measurements are determined for wild type AR0382 or AR0382 $\Delta scf1 + SCF1$ -FLAG mutants encoding the wild type *SCF1* allele or alleles containing the indicated mutations. **(A)** Relative *SCF1* transcript abundance by RT-qPCR compared to wild type AR0382 levels. No significant differences were identified. **(B)** MFI of cells labelled with α -FLAG antibody collected from 50,000 events. No significant differences were identified among strains encoding the various *SCF1* alleles. **(C)** Brightfield and epifluorescent microscopy of cells labeled with α -FLAG antibody. Scale bar = 5 μ m. Statistical differences were assessed using one-way ANOVA with Dunnett's post-hoc test using AR0382 as comparator (A) or AR0382 $\Delta scf1 + SCF1$ -FLAG_{WT} as comparator (B); *p \leq 0.05; **p \leq 0.01; ***p \leq 0.001; ns: p > 0.05.

1130

1135

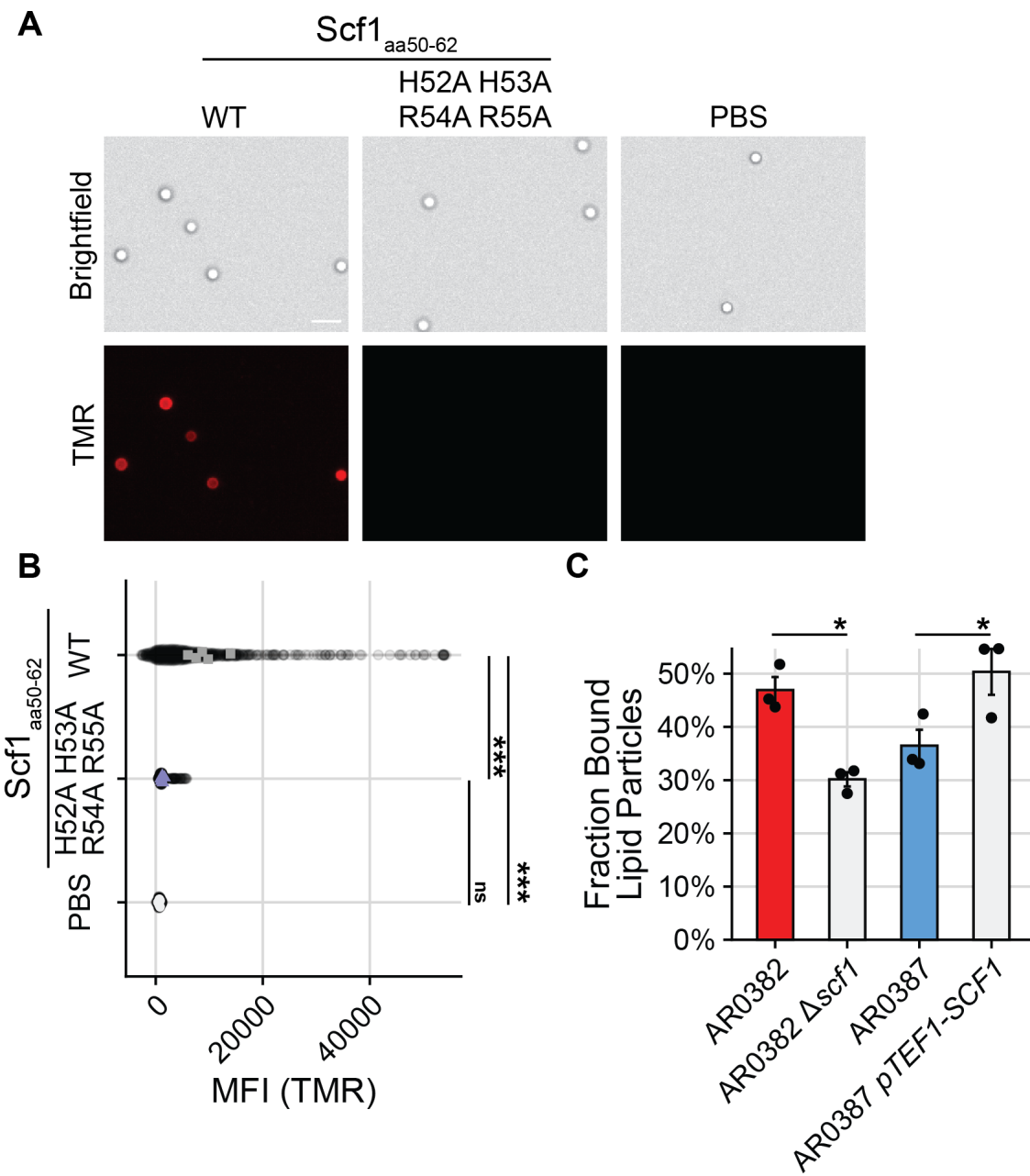


Fig. S12. Scf1 mediates lipid binding. (A) TMR-labelled 13-amino acid peptides corresponding to Scf1 residues 50-62 or the same sequence with indicated mutations were incubated with phosphatidyl choline (PC) microparticles with exposed phospholipid head groups. Scale bar = 10 μm . (B) MFI of PC lipid particles bound by peptides as in (A), normalized to background fluorescence. Each point represents an individual particle. Colored points represent averages from individual experiments, used for statistical analysis. (C) Fraction of PC lipid particles bound by cells after incubation with cultures of each of the indicated strains. Statistical differences were assessed using one-way ANOVA with Tukey's post-hoc test; * $p \leq 0.05$; ** $p \leq 0.01$; *** $p \leq 0.001$; ns: $p > 0.05$.

1140

1145

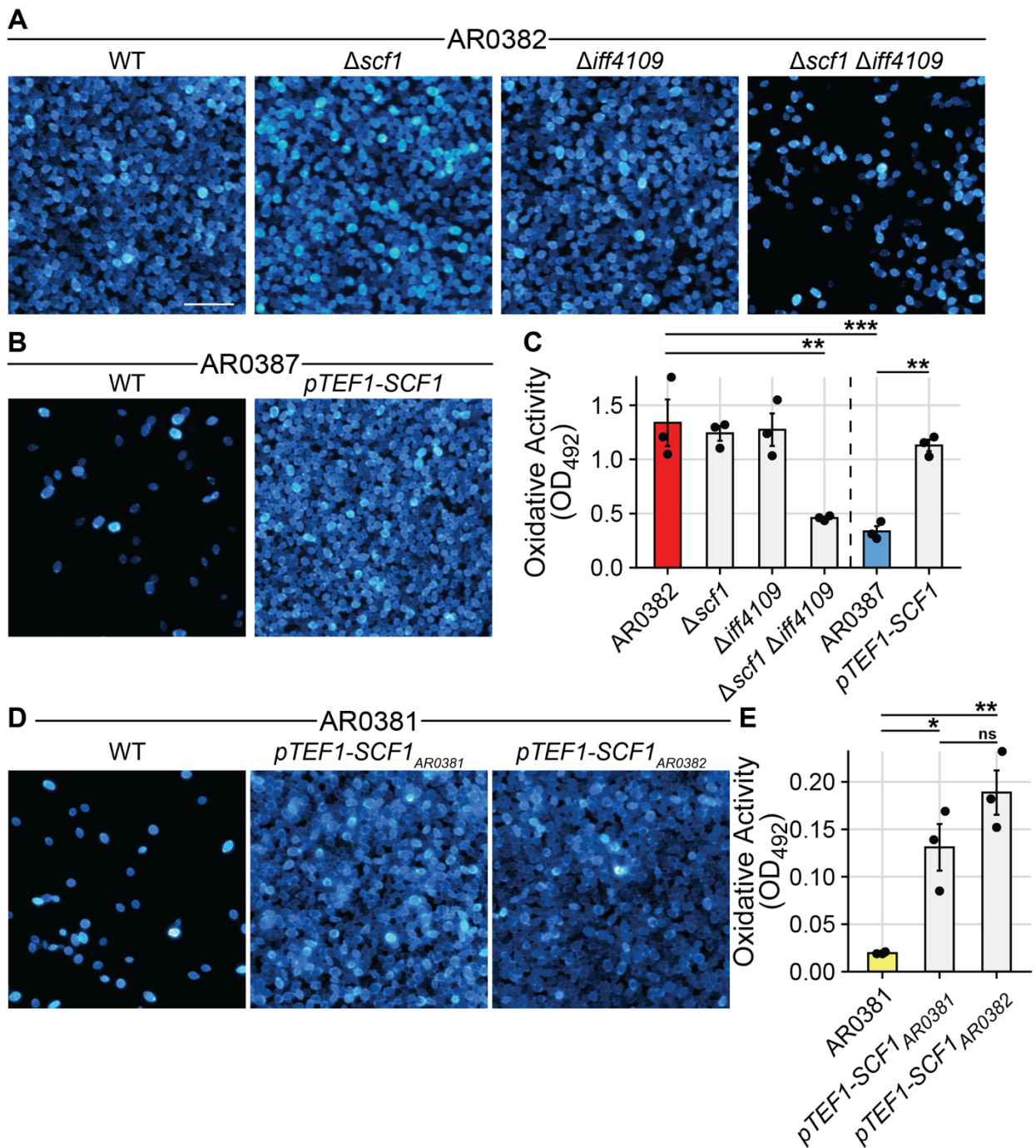


Fig. S13. SCF1 drives biofilm formation *in vitro*. Biofilms were grown on polystyrene in RPMI at 37 °C and stained with calcofluor white. Representative biofilm images in (A), (B), and (D) are depicted as maximum intensity projections from Z-stacks captured using epifluorescence microscopy. (A) Deletion of both *SCF1* and *IFF4109* is required to abrogate biofilm formation in AR0382. (B) Overexpression of *SCF1* is sufficient to drive biofilm formation in AR0387. (C) Oxidative activity of *in vitro* biofilms was measured using an XTT-reduction assay. (D) Expression of *SCF1* in a clade II isolate is sufficient to drive biofilm formation. Representative images of biofilms formed by wild type AR0381 (clade II) or mutants overexpressing either the endogenous AR0381 *SCF1* allele or the clade I *SCF1* allele from AR0382. (E) Oxidative activity of clade II biofilms was measured using an XTT-reduction assay. Scale bar = 20 μm. Statistical

1150

1155

differences were assessed using one-way ANOVA with Tukey's post-hoc test; * $p \leq 0.05$; ** $p \leq 0.01$; *** $p \leq 0.001$; ns: $p > 0.05$.

1160

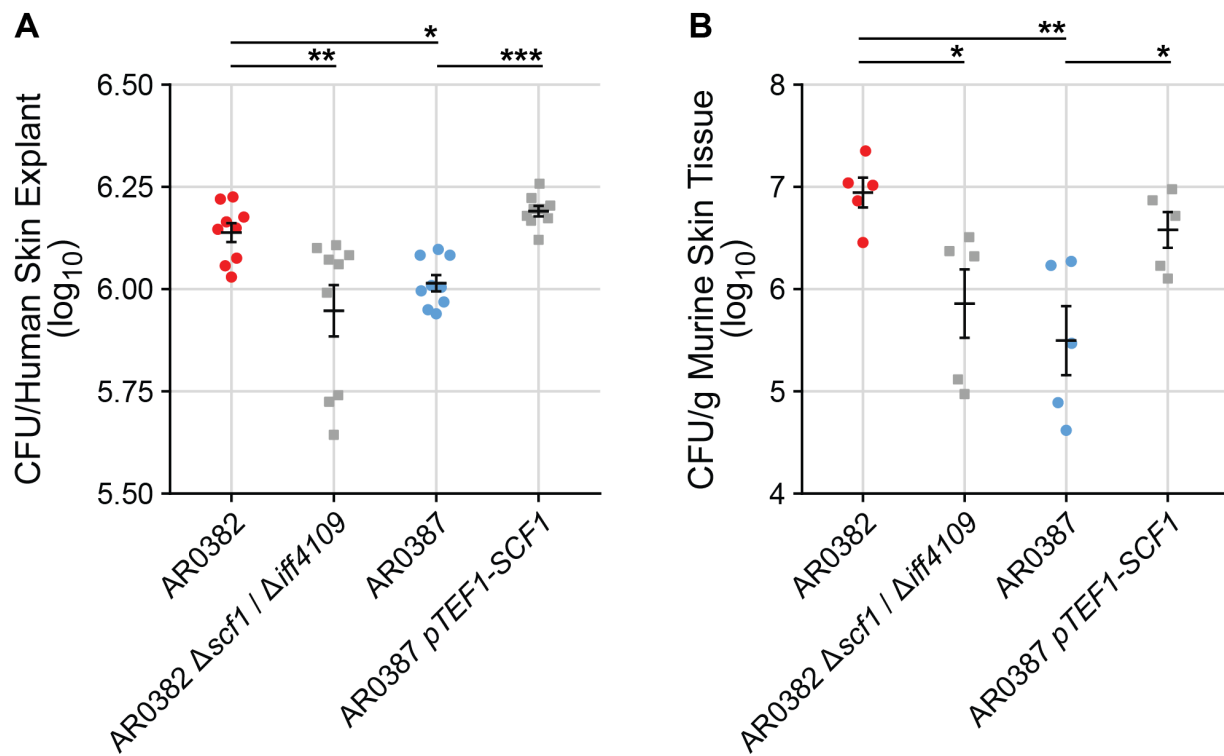


Fig. S14. SCF1 is critical for skin colonization. **(A)** *C. auris* cells were incubated on full thickness *ex vivo* human skin samples for 24 hrs before washing and measuring remaining bioburden by colony forming units (CFU). **(B)** Viable burden of *C. auris* after 2 days incubation on murine skin *in vivo*. Data are presented as CFU/g tissue normalized to actual delivered inocula. Statistical differences were assessed using one-way ANOVA with Tukey's post-hoc test; * $p \leq 0.05$; ** $p \leq 0.01$; *** $p \leq 0.001$; ns: $p > 0.05$.

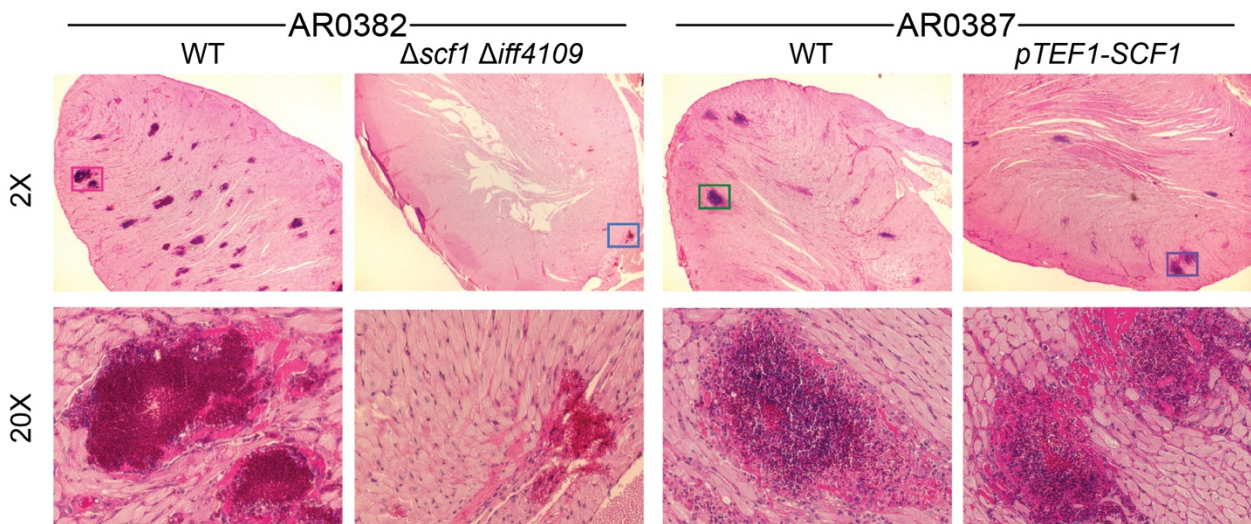


Fig. S15. *SCF1* is critical for dissemination and fungal burden. Histopathology sections of the heart of *C. auris*-infected mice were stained with PAS and imaged at 2X and 20X resolution using Olympus bright field microscopy. Lower panel for each organ represents the magnified area of colored boxes from 2X panel. Magenta color indicates lesion areas.

1175

Table S1.

Strain	Clade	NT Domain % Identity	NT TR Domain Number of Repeats	CT TR Domain Number of Repeats	C Domain % Identity
B8441	I	Ref.	42	46	Ref.
B11220	II	100%	47	31	100%
B11221	III	100%	42	40	92%
B11243	IV	99.6%	42	39	85%
IFRC2087	V	99.6%	35	34	97.7%
B11889	<i>C. haemulonii</i>	60.9%			40.6%

Primary sequence comparison between *SCF1* encoded by *C. auris* strains from each of the five clades and *C. haemulonii*. NT = N-terminal. CT = C-terminal. TR = Tandem Repeat.

Table S2.

Family	Adhesin	Organism	Uniprot ID	Domain Length	Arg (%)	Arg + Lys (%)
<i>SCF1</i>						
	Scf1	<i>C. auris</i>	A0A2H1A319	228	18 (7.9%)	33 (14.5%)
<i>FLO11</i>						
	Flo11	<i>S. cerevisiae</i>	P08640	177	0 (0%)	5 (2.8%)
	KpFLO11	<i>K. pastoris</i>	C4R2D7	171	2 (1.2%)	15 (8.8%)
	Rbt1	<i>C. albicans</i>	Q59TP1	278	5 (1.8%)	26 (9.4%)
<i>PA14</i>						
	Flo1	<i>S. cerevisiae</i>	P32768	176	0 (0%)	4 (2.3%)
	Flo5	<i>S. cerevisiae</i>	P38894	176	0 (0%)	3 (1.7%)
	Flo9	<i>S. cerevisiae</i>	P39712	176	0 (0%)	4 (2.3%)
	Flo10	<i>S. cerevisiae</i>	P36170	161	2 (1.2%)	11 (6.8%)
	Epa1	<i>C. glabrata</i>	Q6FUW5	148	5 (3.4%)	11 (7.4%)
	Epa6	<i>C. glabrata</i>	Q6FX55	159	5 (3.1%)	12 (7.5%)
	Epa9	<i>C. glabrata</i>	B4UMX2	163	5 (3.1%)	16 (9.8%)
	Pwp7	<i>C. glabrata</i>	Q6FQ10	174	4 (2.3%)	12 (6.9%)
	Cea1	<i>K. pastoris</i>	A0A1B2J5V1	161	5 (3.1%)	15 (9.3%)
	KpFlo2	<i>K. pastoris</i>	A0A1B2JGH2	188	9 (4.8%)	12 (6.4%)
<i>ALS</i>						
	Als1	<i>C. albicans</i>	Q5A8T4	247	2 (0.8%)	13 (5.3%)
	Als3	<i>C. albicans</i>	Q59L12	247	3 (1.2%)	14 (5.7%)
	Als9	<i>C. albicans</i>	A0A1D8PQ86	246	2 (0.8%)	11 (4.5%)
	Sag1	<i>S. cerevisiae</i>	P20840	107	1 (0.9%)	2 (1.9%)
	Als2582	<i>C. auris</i>	A0A2H0ZWS7	254	7 (2.8%)	13 (5.1%)
	Als4498	<i>C. auris</i>	A0A2H0ZFP2	254	7 (2.8%)	18 (7.1%)
	Als4112	<i>C. auris</i>	A0A2H0ZH9	255	4 (1.6%)	11 (4.3%)
<i>IFF/HYR</i>						
	Hyr1	<i>C. albicans</i>	Q5AL03	324	10 (3.1%)	26 (8.0%)
	Iff4	<i>C. albicans</i>	Q5AAL9	319	9 (2.8%)	19 (6.0%)
	Iff4109	<i>C. auris</i>	A0A2H0ZI42	312	5 (1.6%)	13 (4.2%)
	Iff1531	<i>C. auris</i>	A0A2H0ZYK9	315	5 (1.6%)	10 (3.2%)
	Iff4892	<i>C. auris</i>	A0A2H0ZGW1	312	3 (1%)	9 (2.9%)

The *SCF1* N-terminal domain is enriched in arginine and lysine residues compared to characterized yeast adhesins. Total residue counts and proportions of arginine and lysine residues from the N-terminal domain of representative adhesins from major yeast adhesin families are shown.

Table S3.

Strain Name	Alias	Genotype	Source
CauTO33	<i>C. auris</i> B11109	AR0382	(50)
CauTO186	<i>C. auris</i> B11109	AR0382 $\Delta als(B9J08_002582)::NAT$	This Study
CauTO187	<i>C. auris</i> B11109	AR0382 $\Delta als(B9J08_004498)::NAT$	This Study
CauTO226	<i>C. auris</i> B11109	AR0382 $\Delta als(B9J08_004112)::NAT$	This Study
CauTO233	<i>C. auris</i> B11109	AR0382 $\Delta iff(B9J08_004100)::NAT$	This Study
CauTO234	<i>C. auris</i> B11109	AR0382 $\Delta iff(B9J08_004109)::NAT$	This Study
CauTO235	<i>C. auris</i> B11109	AR0382 $\Delta iff(B9J08_004098)::NAT$	This Study
CauTO236	<i>C. auris</i> B11109	AR0382 $\Delta iff(B9J08_004110)::NEO$	This Study
CauTO247	<i>C. auris</i> B11109	AR0382 $\Delta iff(B9J08_001531)::NAT$	This Study
CauTO248	<i>C. auris</i> B11109	AR0382 $\Delta iff(B9J08_004892)::NAT$	This Study
CauTO249	<i>C. auris</i> B11109	AR0382 $\Delta iff(B9J08_001155)::NAT$	This Study
CauTO250	<i>C. auris</i> B11109	AR0382 $\Delta iff(B9J08_004451)::NAT$	This Study
CauTO251	<i>C. auris</i> B11109	AR0382 $\Delta iff(B9J08_000675)::NAT$	This Study
At pTO131	<i>Agrobacterium tumefaciens</i> EHA105	EHA105 harboring pTO128 (pPZP-NAT)	(52)
CauTO219	<i>C. auris</i> B11109	AR0382 $tnSWI1(B9J08_003460)$	This Study
CauTO322	<i>C. auris</i> B11109	AR0382 $tnBCY1(B9J08_002818)$	This Study
CauTO261	<i>C. auris</i> B11109	AR0382 $\Delta scf1(B9J08_001458)::NAT$	This Study
CauTO320	<i>C. auris</i> B11109	AR0382 $\Delta scf1(B9J08_001458)::NAT + NAT::SCF1-FLAG NEO$	This Study
CauTO307	<i>C. auris</i> B11109	AR0382 $\Delta iff(B9J08_004109)::NAT + IFF(B9J08_004109) NEO$	This Study
CauTO270	<i>C. auris</i> B11109	AR0382 $\Delta scf1(B9J08_001458)::NAT \Delta iff(B9J08_004109)::NEO$	This Study
CaTO1	<i>C. albicans</i> SC5314	SC5314	
CaTO227	<i>C. albicans</i> SC5314	SC5314 $als1::FRT/als1::FRT$	This Study
CauTO436	<i>C. auris</i> B11109	AR0382 $pTEF1-ALS4112 NAT$	This Study
CauTO32	<i>C. auris</i> B11220	AR0381	(50)
CauTO34	<i>C. auris</i> B11221	AR0383	(50)
CauTO35	<i>C. auris</i> B11222	AR0384	(50)
CauTO36	<i>C. auris</i> B11244	AR0385	(50)
CauTO37	<i>C. auris</i> B11245	AR0386	(50)
CauTO38	<i>C. auris</i> B8441	AR0387	(50)
CauTO39	<i>C. auris</i> B11098	AR0388	(50)
CauTO40	<i>C. auris</i> B11203	AR0389	(50)
CauTO41	<i>C. auris</i> B11205	AR0390	(50)
CauTO52	<i>C. auris</i> B11243	AR0931	(50)
CauTO53	<i>C. auris</i> IFRC2087	AR1097	(50)
CauTO325	<i>C. auris</i> B14308	AR1099	(50)
CauTO326	<i>C. auris</i> B13463	AR1100	(50)
CauTO327	<i>C. auris</i> B18578	AR1101	(50)
CauTO328	<i>C. auris</i> B17835	AR1102	(50)
CauTO329	<i>C. auris</i> B18683	AR1103	(50)
CauTO330	<i>C. auris</i> B18017	AR1104	(50)

CauTO331	<i>C. auris</i> B11842	AR1105	(50)
CauTO315	<i>C. auris</i> A.04.TO.Ax.9-ORG1	Chicago-1	(77)
CauTO316	<i>C. auris</i> A.04.TO.Ax.9-ORG2	Chicago-2	(77)
CauTO317	<i>C. auris</i> B.02.TO.lc.9-ORG1	Chicago-3	(77)
CauTO318	<i>C. auris</i> B.06.TO.Ax.9-ORG1	Chicago-4	(77)
CaTO380	<i>C. albicans</i> P75010	P75010	ATCC
CaTO382	<i>C. albicans</i> 12C	12C	ATCC
CaTO381	<i>C. albicans</i> 19F	19F	ATCC
CaTO388	<i>C. albicans</i> L26	L26	ATCC
CaTO391	<i>C. albicans</i> P37005	P37005	ATCC
CaTO383	<i>C. albicans</i> P37037	P37037	ATCC
CaTO392	<i>C. albicans</i> P37039	P37039	ATCC
CaTO384	<i>C. albicans</i> P78048	P78048	ATCC
CaTO377	<i>C. albicans</i> P94015	P94015	ATCC
CaTO379	<i>C. albicans</i> P76055	P76055	ATCC
CaTO389	<i>C. albicans</i> P76067	P76067	ATCC
CaTO378	<i>C. albicans</i> P34048	P34048	ATCC
CaTO386	<i>C. albicans</i> P57055	P57055	ATCC
CaTO390	<i>C. albicans</i> P78042	P78042	ATCC
CaTO375	<i>C. albicans</i> GC75	GC75	ATCC
CaTO376	<i>C. albicans</i> P600002	P600002	ATCC
CaTO385	<i>C. albicans</i> P75016	P75016	ATCC
CaTO387	<i>C. albicans</i> P75063	P75063	ATCC
CaTO393	<i>C. albicans</i> P87	P87	ATCC
ChTO46	<i>C. haemulonii</i> B10441	AR0395	(50)
ChTO346	<i>C. haemulonii</i> B10441	AR0395 $\Delta scfI(CXQ85_003100)::NAT$	This Study
CauTO306	<i>C. auris</i> B11109	AR0382 $\Delta scfI(B9J08_001458)::NAT$ + $NAT::SCF1_{NEO}$	This Study
CauTO364	<i>C. auris</i> B11109	AR0382 $\Delta scfI(B9J08_001458)::NAT$ + $NAT::SCF1_{Ch}(CXQ85_003100)_{NEO}$	This Study
ChTO324	<i>C. haemulonii</i>	AR0932	(50)
ChTO44	<i>C. haemulonii</i>	AR0393	(50)
CauTO312	<i>C. auris</i> B11220	AR0381 $pTEF1-SCF1_{AR0381}_{NAT}$	This Study
CauTO323	<i>C. auris</i> B11220	AR0381 $pTEF1-SCF1_{AR0382}_{NAT}$	This Study
CauTO438	<i>C. auris</i> B11220	AR0382 $\Delta scfI(B9J08_001458)::NAT$ + $NAT::SCF1_{AR0381}(CJI96_0001187)_{NEO}$	This Study
CauTO308	<i>C. auris</i> B8441	AR0387 $pTEF1-SCF1_{NAT}$	This Study
CauTO432	<i>C. auris</i> B8441	AR0382 $\Delta scfI(B9J08_001458)::NAT$ + $NAT::SCF1-FLAG_{R178A_{K181A}}_{NEO}$	This Study

CauTO433	<i>C. auris</i> B8441	AR0382 $\Delta scfI(B9J08_001458)::NAT + NAT::SCF1-FLAG_{K163A} NEO$	This Study
CauTO434	<i>C. auris</i> B8441	AR0382 $\Delta scfI(B9J08_001458)::NAT + NAT::SCF1-FLAG_{K147A\ R148A\ K150A\ K152A} NEO$	This Study
CauTO430	<i>C. auris</i> B8441	AR0382 $\Delta scfI(B9J08_001458)::NAT + NAT::SCF1-FLAG_{R54A\ R55A} NEO$	This Study
CauTO453	<i>C. auris</i> B8441	AR0382 $\Delta scfI(B9J08_001458)::NAT + NAT::SCF1-FLAG_{H52A\ H53A\ R54A\ R55A} NEO$	This Study
CauTO455	<i>C. auris</i> B8441	AR0382 $\Delta scfI(B9J08_001458)::NAT + NAT::SCF1-FLAG_{K44A\ H55A\ Y46A\ W47A\ K49A} NEO$	This Study

Strains used in this study.

Table S4.

Name	Description	Source
pTO135	<i>pENO1-CaCas9-tCyc1, AMP</i>	(52)
pTO136	<i>pADH1-tRNA-Ala-gRNA-tracrRNA-HDV-tAgTEF2, AMP</i>	(52)
pTO137	<i>RFP-tADH1-pAgTEF2-NAT1-tAGTEF2, AMP</i>	(52)
pTO169	<i>ACE2 NEO, AMP</i>	(52)
pTO139	<i>pUC19, AMP</i>	(52)
pTO144	<i>als(B9J08_002582)::NAT, AMP</i>	This Study
pTO167	<i>als(B9J08_004498)::NAT, AMP</i>	This Study
pTO166	<i>als(B9J08_004112)::NAT, AMP</i>	This Study
pTO145	<i>iff(B9J08_004100)::NAT, AMP</i>	This Study
pTO148	<i>iff(B9J08_004109)::NAT, AMP</i>	This Study
pTO202	<i>iff(B9J08_004098)::NAT, AMP</i>	This Study
pTO188	<i>iff(B9J08_004110)::NEO, AMP</i>	This Study
pTO146	<i>iff(B9J08_001531)::NAT, AMP</i>	This Study
pTO147	<i>iff(B9J08_004892)::NAT, AMP</i>	This Study
pTO205	<i>iff(B9J08_001155)::NAT, AMP</i>	This Study
pTO206	<i>iff(B9J08_004451)::NAT, AMP</i>	This Study
pTO207	<i>iff(B9J08_000675)::NAT, AMP</i>	This Study
pTO222	<i>IFF(B9J08_004109) NEO, AMP</i>	This Study
pTO211	<i>scf1::NAT, AMP</i>	This Study
pTO221	<i>iff(B9J08_004109)::NEO, AMP</i>	This Study
pTO100	<i>pLC49 C. albicans NAT flp</i>	(51)
pTO102	<i>pLC953 C. albicans Cas9 sgRNA</i>	(51)
pTO288	<i>pTEF1-ALS(B9J08_004112), NAT, AMP</i>	This Study
pTO255	<i>scf1(CXQ85_003100)::NAT, AMP</i>	This Study
pTO264	<i>SCF1Ch (CXQ85_003100) NEO</i>	This Study
pTO250	<i>pTEF1-SCF1 NAT, AMP</i>	This Study
pTO223	<i>SCF1 NEO, AMP</i>	This Study
pTO284	<i>SCF1AR0381 (CJI96_0001187) NEO, AMP</i>	This Study
pTO280	<i>SCF1-FLAG NEO, AMP</i>	This Study
pTO281	<i>SCF1-FLAGK163A NEO, AMP</i>	This Study
pTO282	<i>SCF1-FLAGK147A R148A K150A K152A NEO, AMP</i>	This Study
pTO283	<i>SCF1-FLAGR54A R55A NEO, AMP</i>	This Study
pTO268	<i>SCF1-FLAGR178A K181A NEO</i>	This Study
pTO292	<i>SCF1-FLAGH52A H53A R54A R55A NEO</i>	This Study
pTO293	<i>SCF1-FLAGK44A H55A Y46A W47A K49A NEO</i>	This Study

1190

Plasmids used in this study.

Table S5.

Name	Sequence	Purpose
qPCR Primers		
oTO359	CGTGCTGTGTTCCCATCCAT	<i>C. auris ACT1</i>
oTO360	AGCCTCATCACCGACATAACG	
oTO1251	GTGAGAGTGGAGTCGGAACG	<i>C. auris SCF1</i>
oTO1252	CAGCTTCTCCTCTGGCTCC	
oTO615	GGGAGACACCTTGACGCTT	<i>IFF</i> (B9J08 004109)
oTO616	GTTGGCTCAGGGAAAGTCGAA	
oTO1253	TGAGAGATTAGAGGCCCG	<i>C. haemulonii ACT1</i>
oTO1254	TACGCTCTGCAATACCTGGG	
oTO1229	TTGGTGAAGGAGCAACCGAG	<i>C. haemulonii SCF1</i>
oTO1230	GGGGCTTCAAGTGTCTGACT	
Amplification of transformation cassettes		
oTO143	CCTTTGTAGTTCAACTTATGC	Amplification of Cas9 Cassette
oTO41	GTCCCCAAAACCTTCTCAAGC	
oTO18	CAGGAAACAGCTATGAC	Amplification of Repair Cassettes
oTO19	GTAAAACGACGGCCAG	
oTO1159	gactacaaggacgacgtgacaagACAACCACCACTACTCG	Overlap Extension PCR for <i>SCF1-FLAG</i> Cassette
oTO1160	cttgcattcgccgttagtcTTCACACTCACACACCCAAC	
oTO224	GCTATTACGCCAGCTGG	pTO222 Repair Cassette
oTO225	CGCAATTAAATGTGAGTTAGC	
oTO945	CAGTGGAGCGGAAACTC	pTO250 Repair Cassette
oTO946	GTGGACCTGATTGACTGG	
oTO947	CCTGAATCTCTAACGAAAG	pTO222 Repair Cassette
oTO948	GTGGTGTAAAGCGATTGTG	
oTO1161	GCAAGACGAACCTCCAAC	
Amplification of plasmid fragments for Gibson Assembly		
oTO590	GGATCCTCTAGAGTCGAC	Amplification of pUC19 backbone
oTO591	GGTACCGAGCTCGAATTTC	
oTO668	ACTGGATGGCGGCCGTTAG	Amplification of NEO cassette
oTO669	CGACATGGAGGCCAGAACAT	
oTO874	ATCAAGCTTGCCTCGTCC	Amplification of NAT cassette
oTO184	ttcgagctcggtaccGTACTCATCAGAGTATACGATGC	Assembly of pTO144
oTO185	acggccgccatccagtGAGCAGTCGATGCTCAAATTAATC	
oTO186	aagcatcgactgctcACTGGATGGCGGCCGTTAG	
oTO187	gagaacctaataattATCAAGCTTGCCTCGTCC	
oTO188	cgaggcaagctgtatTTTAGGTTCTCTAGCC	
oTO189	gactctagaggatcccGGAGTGTACATTCTTTC	
oTO190	aaatgtacactccGGATCCTCTAGAGTCGAC	
oTO191	tactctgtatgatGGTACCGAGCTCGAATT	
oTO410	TAGCCTTGATTGAGCAACCGGATCCTCTAGAGTCGACCT	Assembly of pTO167
oTO411	TACAAATAGCAGTTATCAGCGGTACCGAGCTCGAATTAC	
oTO412	GTGAATTGAGCTCGGTACCGCTGATAACTGCTATTGTATACA	
oTO413	taactaacggccatccagtTGATAAATGGAAAGTAGAGAACAT	
oTO414	TCTCTACTTCCATTATCAactggatggccggcgtagta	
oTO415	AAATAATAATTGAGTAGGCCatcaagttgcctcgcc	
oTO416	ggacgaggcaagctgtatGGCCTACTCAATTATTATTTAATT	
oTO417	AGGTCGACTCTAGAGGATCCGGTTGCTCAAATCAAGGCTA	
oTO402	GAATCCTGAAAACGCTTGGGATCCTCTAGAGTCGACCT	
oTO403	GCGTTACGGCGATTGCACCGGTACCGAGCTCGAATTAC	
oTO404	GTGAATTGAGCTCGGTACCGGTGCAATGCCGTAAACGC	

oTO405	tactaacgcggccatccagtGAAAGATGATGGGAAACAAGGTGA	Assembly of pTO166
oTO406	CTTGTTCATCCTTCactggatggcgccgttagta	
oTO407	GGTATCATAAAAGCTCACGTatcaagcttgcctcgcc	
oTO408	ggacgaggcaagcttgcACGTGAGCTTTATGATAACCT	
oTO409	AGTCGACTCTAGAGGATCCCAAGCGTTTCAGGATAGTC	
oTO192	ttcgagctcggtaccCCTTCTCGAGTTACTCTG	Assembly of pTO145
oTO193	acgcgcgcattccagtTGGATAAAGCAAGTGAAAAAG	
oTO194	cacttgcttatccaACTGGATGGCGGCCGTAG	
oTO195	agtgggtatatggcATCAAGCTTGCCTCGTCC	
oTO196	cgaggcaagcttgcGACCATAACCCACTCGC	
oTO197	gactctagaggatccGCCACTTACTGCCAAC	Assembly of pTO148
oTO198	gcaagtaagtggcGGATCCTCTAGAGTCGAC	
oTO199	agtaactcgagaaggGGTACCGAGCTCGAATT	
oTO216	ttcgagctcggtaccCAGACATCTTGTGCAAG	
oTO217	acgcgcgcattccagtTTGTTGATGGGAACTAC	
oTO218	gttccccatcaaACTGGATGGCGGCCGTAG	Assembly of pTO202
oTO219	aaagtgcacccgtcaATCAAGCTTGCCTCGTCC	
oTO220	cgaggcaagcttgcTGACGGTGTCACTTCGAG	
oTO221	gactctagaggatccGTGGTGTAAAGCGATTGTG	
oTO222	aatgcattcacaccGGATCCTCTAGAGTCGAC	
oTO223	cacaagatgtctgGGTACCGAGCTCGAATT	
oTO786	acgacggccagtgaattcgagctcggtaccCGTATTCTCGAGCTCTAAAG	Assembly of pTO202
oTO787	acgcgcgcattccagtATGGTTGATTAACAAAAGAAAAAAAAAAAAAAAG	
oTO788	tgttaatcaaccattACTGGATGGCGGCCGTAG	
oTO789	gcttagaaaaattgcATCAAGCTTGCCTCGTCC	
oTO790	cgaggcaagcttgcGCAATTTCCTAGCCTTTATTTC	
oTO791	catgcctgcaggctcgactctagaggatccCTACCAAAAGTTGACGTG	Assembly of pTO188
oTO678	ggccagtgaattcgagctcggtaccGCAAACGTCACTACCG	
oTO679	ttcgatactaaccgcgcgcattccagtGATGGAATGGATGGAGAG	
oTO680	gagggtattctggccatgtcgCTTTAAAATGTTTATTAGTTCTG	
oTO681	cctgcaggctcgactctagaggatccGTACAGCTTACACAACAAATTAC	
oTO200	ttcgagctcggtaccGGTCTTGTAAACATGGCC	Assembly of pTO146
oTO201	acgcgcgcattccagtGATGCTCAATAGCTGAAG	
oTO202	cagctattgagcatcACTGGATGGCGGCCGTAG	
oTO203	aatttgtacgttagATCAAGCTTGCCTCGTCC	
oTO204	cgaggcaagcttgcCCTAACGTACCAATTCTC	
oTO205	gactctagaggatccCCAAAAATATGAAGACGAGAG	Assembly of pTO147
oTO206	tcttcattttggGGATCCTCTAGAGTCGAC	
oTO207	catgttaacaagaccGGTACCGAGCTCGAATT	
oTO208	ttcgagctcggtaccGCAGCTGCATTGGTACATATG	
oTO209	acgcgcgcattccagtGTGGAGCAGGTTGGTAG	
oTO210	ccaaacctgcctcacACTGGATGGCGGCCGTAG	Assembly of pTO205
oTO211	tttgtcatttaagtATCAAGCTTGCCTCGTCC	
oTO212	cgaggcaagcttgcACTTAAATGCACAAACGC	
oTO213	gactctagaggatccGGACTACAGCTTCTGG	
oTO214	aagaagcttgcGGATCCTCTAGAGTCGAC	
oTO215	taccaatgcagctgcGGTACCGAGCTCGAATT	
oTO819	acgttgaaaacgcgcgcaggtaattcgagctcggtaccCAAAGTAGCCACACACTTG	Assembly of pTO205
oTO820	tactaacgcgcgcattccagtATTGGCAGAGAGTAAATG	
oTO821	cattctactctgcattaaACTGGATGGCGGCCGTAG	
oTO822	tgtcaggccatgtcaacaATCAAGCTTGCCTCGTCC	
oTO823	ggggacgaggcaagcttgcTGTGATACAAGGCTGCAC	
oTO824	cgccaaactgcattgcgcgcaggctcgactctagaggatccCTCGCCTCGTGTGG	
oTO825	acgttgaaaacgcgcgcaggtaattcgagctcggtaccGAACGCAACAACCTAAGC	

oTO1066	GTAGCAGCATGATTATGAACAGG	Assembly of pTO223
oTO1077	tgctgtcgattcgatactaacgcgcgcattccagtTTCTAATGACTGATACTCATACTT TC	
oTO1430	TTAAAGCAACAAGGCAGC	Assembly of pTO284
oTO1431	TACACCTGCAAGAAGTAAAGAGAACATCTCATTGTGGAGGTGAAGT TTAAG	
oTO1432	CTTGCTTGCTGCTGCCTGTTAAGTAGCAGCATGATTAT GAAC	Assembly of pTO280
oTO1159	gactacaaggacgacgatgacaagACAACCACCACTACTTCG	
oTO1160	cttgcattcgccctttagtcTTCACACTCACACACCCAAC	Assembly of pTO281
oTO1427	CAGTTAATAGTTGCGCAACG	
oTO1428	CTGTAGCAATGGCAACAAAC	
oTO1417	CCGGCGTTGTGCTGCTCTCCCACATGCTTGGAGGTTCGCTTG CTTGGAGCCAG	Assembly of pTO282
oTO1418	GAACCTCCAAGCATGTGGGAGACAGCACACAACGCCGGCTGG TTTGTGCTTGTGTCTC	
oTO1421	AACGGATGCTCGAGGCTGCTCACGCTCACGCTCCAGCCGGCGTT GTGTGCTGCTCCAC	Assembly of pTO283
oTO1422	CCGGCTGGAGCGTGAGCGTGAGCAGCCTCGAGCATCCGTTCCGA CCTCACTCTCACTCTG	
oTO1425	GCCATCATGCTGCTCCAACGATGGCCCCGAGTTATCGATGCG GGAG	Assembly of pTO292
oTO1426	GGGGCCATCGTTGGAAGCAGCATGATGGCCACTTCACCCAGT AGTG	
oTO1563	GCGCTGCTGCTGCTCCAACGATGGCCCCGAGTTATCGATGCG GGAG	Assembly of pTO293
oTO1564	GGGGCCATCGTTGGAAGCAGCAGCAGCAGCGCCACTTCACCCAGT AGTG	
oTO1565	TGCTGCTGCTGCTGGCTGGTGGCCATCATCGCTGTTCCAAC	Assembly of pTO293
oTO1566	GCCACCAGCCACAGCAGCAGCAGCAGAAGGTGTACAGTAGTCG TC	

1195

Oligonucleotides used in this study.

Data S1. Source Data